Check for updates

International Journal of Climatology

International Journal of Climatology | RMetS

RESEARCH ARTICLE OPEN ACCESS

A Classification of High-Risk Atmospheric Circulation Patterns for Italian Precipitation Extremes

Cristina Iacomino[1] | Salvatore Pascale[1] | Giuseppe Zappa[2] | Marcello Iotti[3] | Federico Grazzini[2,4] | Paolo Ghinassi[2] | Alice Portal[2]

[1]Department of Physics and Astronomy, University of Bologna, Bologna, Italy | [2]Isac, CNR, Bologna, Italy | [3]IMATI, CNR, Genova, Italy | [4]SIMC, ARPAE, Bologna, Italy

Correspondence: Salvatore Pascale (salvatore.pascale@unibo.it)

Received: 14 March 2025 | **Revised:** 1 September 2025 | **Accepted:** 5 September 2025

Funding: This research was supported by the European Union—NextGenerationEU, mission 4 component 1 CUP B53D23006830006. Project Title "Evaluating the changing risk of cyclones for Italian precipitation extremes" (ENCIRCLE).

Keywords: extreme precipitation | Italy | self-organising maps | weather types

ABSTRACT

Precipitation extremes are a significant natural hazard that has caused considerable destruction in Italy over the past decade. However, our understanding of the effects of climate change on these extremes remains incomplete, with unclear trends in the intensity and frequency of precipitation extremes. Part of this uncertainty results from internal variability in atmospheric circulation, which is key in triggering high-impact precipitation events. To address this issue, here we develop a comprehensive classification of the Weather Types (WTs) associated with November 1984 to October 2024 Extreme Precipitation Events (EPEs) from CERRA in the 156 operational warning areas used by the Italian Department of Civil Protection, by applying Self-Organising Maps to sea level pressure and 500 hPa geopotential height. We identify six different WTs associated with Italian EPEs, corresponding to different large-scale dynamical drivers: Atlantic cyclone over France/northern Tyrrhenian Sea (WT1), Mediterranean cyclone over Central Italy (WT2), Western Mediterranean cyclone associated with upper level trough over Iberia (WT3), Westerly zonal flow (WT4), upper-level cut-off low (WT5), and Mediterranean cyclone centered over the Tyrrhenian Sea (WT6). The relevance of these WTs for different warning areas is evaluated through composites of moisture transport, the probability of EPEs given a specific WT and a seasonality analysis. The annual frequency of extreme precipitation events exhibits a statistically significant increasing trend (Mann-Kendall, $p < 0.05$), corresponding to an average rise of more than two additional events per year per decade. The positive trend in precipitation extremes occurs for five out of the six WTs, with the largest increase occurring for WT4. These results add to the existing knowledge of drivers of extreme precipitation events in Italy, providing an understanding of underlying large-scale atmospheric circulation and a database of weather types to investigate the role of anthropogenic climate change in climate model simulations.

1 | Introduction

In recent years, southern Europe has faced extraordinary heavy precipitation events that have caused devastating effects in many areas. On October 29, 2024, the district of Valencia, Spain, was affected by very heavy precipitation, recording 300 mm of daily precipitation in a large area and reaching the record value of 621 mm in 6 h in the town of Turìs (AEMET Agencia Estatal de Meteorología 2024). The subsequent floods caused more than 200 fatalities (Moore et al. 2024; Jones 2024; CBS News 2024). The Emilia-Romagna region in Northern Italy was affected by four heavy precipitation events in less than 17 months (two in May

This is an open access article under the terms of the Creative Commons Attribution License, which permits use, distribution and reproduction in any medium, provided the original work is properly cited.

© 2025 The Author(s). *International Journal of Climatology* published by John Wiley & Sons Ltd on behalf of Royal Meteorological Society.

2023, September 2024, October 2024) causing heavy floods. The most recent occurred on October 19, 2024, with measurements reaching 100 mm of precipitation in 4 h (ARPAE 2024c). The one in September 2024 was associated with Cyclone Boris, which propagated southwestward over the Italian Peninsula after producing torrential rainfall and severe flooding in many areas of Central Europe, including Poland, the Czech Republic, Romania, Slovakia, and Austria (ARPAE 2024a; ECMWF 2024). In Emilia Romagna, Cyclone Boris led to local peaks of 350 mm accumulated precipitation over less than 48 h (ARPAE 2024b). The intensity of these recent events raises questions about the role played by anthropogenic climate change in extreme precipitation events.

Climate change impacts the intensity of precipitation extremes primarily via an increase in atmospheric water vapour content associated with atmospheric warming. This is commonly referred to as the thermodynamical contribution (Trenberth 1999; Allen and Ingram 2002) and approximately scales as the Clausius-Clapeyron relationship, with a relative increase of about 7% per degree of warming (Pall et al. 2007; Hartmann 2016). The Clausius-Clapeyron scaling rate for daily precipitation extremes has been found to be overall consistent with observations and very high-resolution regional climate model simulations for various locations worldwide (Pall et al. 2007; Allen and Ingram 2002; Ban et al. 2020), although super-Clausius-Clapeyron scaling has also been observed in sub-daily extremes and related to a shift from (low-intensity) stratiform to (higher-intensity) convective rainfall regimes (e.g., Ban et al. 2020; Lenderink et al. 2017; Da Silva and Haerter 2025).

Moreover, anthropogenic global warming can affect regional patterns of extreme precipitation also through changes in the atmospheric circulation (O'Gorman and Schneider 2009; O'Gorman 2015). Hence, higher and lower rates of change compared to the Clausius-Clapeyron scaling rate can also be related to dynamical factors (O'Gorman 2015). While the thermodynamic contribution to changes in precipitation extremes is positive and relatively homogeneous in space, the dynamical contribution is spatially heterogeneous (Pfahl et al. 2017) and can dominate on a regional scale (Shepherd 2014; Seneviratne et al. 2021). Since different global climate models tend to disagree in their dynamical response, the dynamics represent a major source of uncertainty in precipitation extreme projections at the regional and seasonal scale (Shepherd 2014; Pfahl et al. 2017; John et al. 2022). This is the case for the Mediterranean region, where the IPCC reports low confidence on the response of extreme precipitation events to climate change (Seneviratne et al. 2021; Pfahl et al. 2017). In addition to that, the complex orography of the Mediterranean region further modulates the signal and introduces additional modelling complexity which increases the variability in future precipitation projections (e.g., Giorgi et al. 2016).

In synoptic climatology and meteorology, the concepts of atmospheric circulation type or Weather Type (WT hereafter; Beck and Philipp 2010, Casado and Pastor 2016, Philipp et al. 2010, Huth et al. 2016, Ramos et al. 2015, Vallorani et al. 2018), weather regime (e.g., Michelangeli et al. 1995) and atmospheric circulation analogue (Lorenz 1969; Yiou et al. 2007) have been applied to study synoptic conditions that favour high precipitation events (e.g., Nuissier et al. 2011; Grazzini et al. 2020; Capozzi et al. 2023; Mastrantonas et al. 2022) and in studies of detection and attribution of anthropogenic climate change signals (e.g., Yiou et al. 2007; Vautard and Yiou 2009). WTs can serve as a valuable tool, as they can summarise the variability in the atmospheric circulation into a restricted number of discrete classes or patterns, allowing for an effective description of atmospheric circulation (Iannuccilli et al. 2021). Circulation types also act as mediators between long-range teleconnections and local-scale impact-related variables by modulating how large-scale climate signals translate into regional weather patterns (Spuler et al. 2024; Dorrington, Grams, et al. 2024). In the past decade, the concept of circulation types and analogues has proven useful in distinguishing the dynamic and thermodynamic contributions of climate change in extreme events (e.g., Vautard et al. 2016; Yiou et al. 2017). Precipitation extremes in a given region are linked to specific WTs and local thermodynamic environments that interact, producing these events.

Accurately classifying the WTs associated with extreme precipitation in Italy represents a valuable step for better assessing the impact of anthropogenic climate change on precipitation extremes in the Italian peninsula. This includes dynamical contributions, such as changes in the frequency and characteristics of these weather types, and thermodynamical contributions, that is changes in the moisture and temperature environment for a given WT.

Atmospheric circulation types over Italy associated with heavy precipitation have been investigated in previous studies, although these were either focused on specific Italian regions or based on precipitation observations from a limited number of stations (Grazzini et al. 2020; Capozzi et al. 2023; Federico et al. 2008; Mastrantonas et al. 2022; Iannuccilli et al. 2021). Using the ArCIS dataset (Pavan et al. 2013), Grazzini et al. (2020) classified extreme precipitation events (EPEs) over North-Central Italy into three different dynamical classes: events primarily caused by frontal/orographic uplift ("Cat1"); events resulting from frontal uplift with embedded (equilibrium) deep convection ("Cat2"); events primarily produced by deep convection ("Cat3"). Federico et al. (2008), Mastrantonas et al. (2022) and Capozzi et al. (2023) investigated atmospheric circulation patterns associated with heavy rainfall in specific regions of Southern Italy (i.e., Calabria the first two studies and Campania the latter, respectively) using precipitation data from meteorological stations. Analysing 8 years of data (1999–2007), Federico et al. (2008) identified 11 atmospheric circulation types, while Mastrantonas et al. (2022) applied nine Mediterranean patterns previously identified in Mastrantonas et al. (2021) over the Calabria region for forecasting purposes, and Capozzi et al. (2023) considered a 20-year (2002–2021) dataset, obtaining six precipitation clusters. Iannuccilli et al. (2021) used precipitation data from 46 weather stations scattered across the entire Italian peninsula to analyse the relation between precipitation data and large-scale circulation patterns. Their weather type classification is very much restricted over an Italian domain (i.e., 5E—20E, 35 N- 50 N), which makes it difficult to appreciate the relationship of these patterns with the large-scale atmospheric circulation over the Atlantic-European sector, to which Italian weather is inextricably linked (e.g., Miglietta and Davolio 2022).

The goal of this work is to provide a general classification of the large-scale atmospheric circulation types associated with heavy precipitation events over the entire Italian peninsula,

10970088, 2025, 15, Downloaded from https://rmets.onlinelibrary.wiley.com/doi/10.1002/joc.70118 by CochraneItalia, Wiley Online Library on [03/12/2025]. See the Terms and Conditions (https://onlinelibrary.wiley.com/terms-and-conditions) on Wiley Online Library for rules of use; OA articles are governed by the applicable Creative Commons License

extending the scope of previous studies. However, high-quality gridded datasets of observed precipitation covering all of Italy are lacking. To address this limitation, we use two state-of-the-art precipitation datasets, CERRA and MSWEP, and evaluate their suitability for studying EPEs in Italy by comparing them against the high-quality ArCIS observational dataset available for North-Central Italy. Based on this assessment, we then create an event set of EPEs across the entire Italian domain. Finally, we identify the dominant circulation patterns associated with these extremes by applying Self-Organising Maps (SOMs; Kohonen 1982) to geopotential height at 500 hPa (Z500) and mean sea level pressure (mSLP) retrieved from the ERA5 reanalysis. The SOM method is an unsupervised machine learning model widely used in synoptic climatology (e.g., Hewitson and Crane 2002; Liu and Weisberg 2011; Sheridan and Lee 2011; Givon et al. 2024). The classification has the potential to be applied, in future studies, to climate model simulations in order to disentangle the dynamic and thermodynamic drivers of changes in precipitation extremes over Italy.

The manuscript is structured as follows. In Section 2, we discuss the different precipitation and atmospheric datasets used in this study, along with the SOM-based approach employed for characterising weather types; in Section 3 we present the weather types obtained from our SOM-based method and describe their key synoptic and dynamical features; finally, Section 4 examines the main findings within the context of recent literature, while Section 5 concludes the manuscript and outlines directions for future research.

2 | Data and Methods

2.1 | Datasets

To identify EPEs, we use three gridded precipitation datasets, ArCIS, CERRA, and MSWEP.

ArCIS (*Archivio Climatologico per l'Italia Settentrionale*, Climatological Archive for Central–Northern Italy; Pavan et al. 2013, 2019), version 3.0, is a daily precipitation dataset for North-Central Italy (Figure 1a) at 0.06305°×0.045° spatial resolution (approximately 5 km×5 km) extending from 1961 to the present. ArCIS is based on observations from 850 rain gauges of 11 Italian regions, plus some foreign stations to appropriately cover the Alpine borders. All are subject to quality check, synchronisation, analyses of time consistency and statistical homogeneity. Interpolation is applied using a modified Shepard scheme (Antolini et al. 2016; Pavan et al. 2019). For the period 1961 to 2015 the 24-h accumulation period is from 9 a.m. on one day to 9 a.m. local time on the following day in Italy, which corresponds to 08-08UTC in Central European Time (CET) and 07-07UTC in Central European Summer Time (CEST). For the subset of the dataset from 2016 to 2019, the accumulation period is instead 0 UTC to 24 UTC. Timestamps have been arranged so that they always correspond to the day at the start of the accumulation period (cf. Grazzini et al. (2020)).

CERRA (the Copernicus European Regional ReAnalysis; Ridal et al. 2024) is a high-resolution regional reanalysis dataset at 5.5 km×5.5 km featuring a finer spatial resolution than ERA5, from which it inherits its initial and lateral boundary conditions. CERRA is characterised by a temporal coverage from September 1984 to October 2024. CERRA combines model data with observations through a 3-dimensional variational data assimilation scheme of the atmospheric state at every assimilation time (Schimanke et al. 2021). Daily total precipitation from 06 to 06 UTC has been obtained by combining forecasts initialised at 00 UTC and 12 UTC, and lead times from 6 to 18 h. The first 6 h of each forecasts are not considered to reduce the influence of model spin-up. Using `cdo remapcon` we conservatively remapped the data, which was originally in a conformal Lambert grid, on a regular at 0.06305°×0.05° grid of nearly equivalent

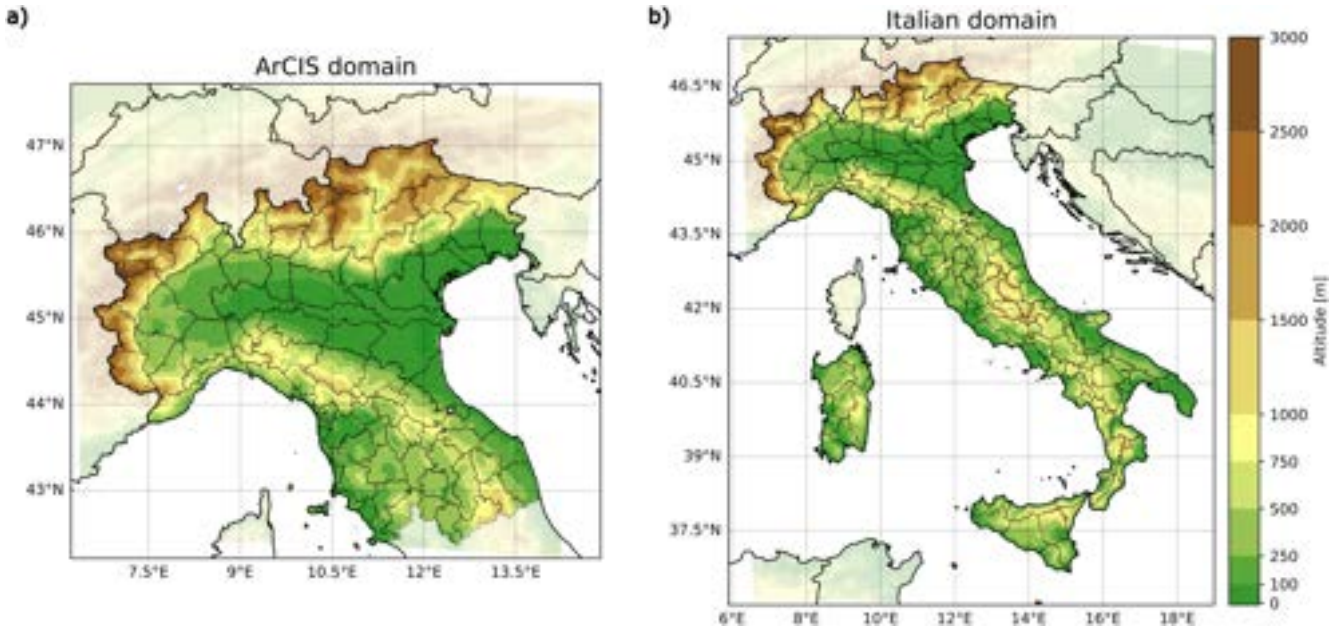

FIGURE 1 | (a) The 94 operational warning areas of North-Central Italy, and (b) the 156 warning areas for the entire peninsula. Warning areas are operational regions used by the Italian Department of Civil Protection for the national warning system. The terrain elevation of the region is represented by shaded colours.

10970088, 2025, 15, Downloaded from https://rmets.onlinelibrary.wiley.com/doi/10.1002/joc.70118 by CochraneItalia, Wiley Online Library on [03/12/2025]. See the Terms and Conditions (https://onlinelibrary.wiley.com/terms-and-conditions) on Wiley Online Library for rules of use; OA articles are governed by the applicable Creative Commons License

resolution, in order to facilitate the computation of area-averages of precipitation over warning areas (Section 2.2.1).

MSWEP (GloH2O 2020) is a 0.1°×0.1° resolution precipitation dataset with global coverage, spanning the period 1979-present and providing precipitation at 3-hourly frequency. MSWEP integrates gauge, satellite, and reanalysis data, thus increasing its performance in densely gauged, convection-dominated, and frontal-dominated regions (Beck, Hylke & National Center for Atmospheric Research Staff 2023). In this study we used the "Past" variant of MSWEP—which incorporates daily gauge observations—over 1985–2019. We accumulated precipitation to obtain daily totals from 06-06 UTC in order to have the same accumulation period as CERRA and to allow a fair comparison of the two datasets with ArCIS.

To analyse the atmospheric circulation associated with EPEs we examine geopotential height at 500 hPa (Z500), mean sea level pressure (mSLP), total column water vapour (TCWV) and integrated vapour transport (IVT) from ERA5 (Hersbach et al. 2020), the latest ECMWF global atmospheric reanalysis, covering the time period 1940-present. ERA5 precipitation is only briefly examined as a consequence of its coarser resolution. In fact, it tends to underestimate extreme precipitation (Lavers et al. 2022) and smooth local maxima (Bandhauer et al. 2022; Cavalleri et al. 2024), especially in areas with significant orography such as the Italian peninsula. Moreover, its 0.25°×0.25° horizontal spatial resolution does not suite the analysis of precipitation at the scale of individual warning areas, since some areas do not contain any ERA5 grid points. Atmospheric fields are analysed over two geographical domains: a large European domain (60° N-25° N, 13° W-35° E), to have a large-scale picture of the atmospheric circulation patterns linked to EPEs, and a regional Italian domain (5° E—19° E, 36° N—48° N) emphasising regional moisture transport.

For the initial part of the analysis, which involves inter-dataset comparison, we consider the time period 1985 to 2019, corresponding to the temporal overlap among the datasets. Subsequently, the analysis is extended to the longest available period (November 1984–October 2024), reaching as close as possible to the present, while considering only complete years. This choice is motivated by a sensitivity analysis (not shown), which found that including incomplete years would bias the resulting patterns due to seasonal under- or over-representation.

2.2 | Methods

2.2.1 | Definition of Extreme Precipitation Event (EPE)

Following Grazzini et al. (2020), we first compute the area-averaged daily precipitation over each operational Warning Area (WA) defined by the Italian Department of Civil Protection (Figure 1). We then define an extreme precipitation event (EPE) when the area-averaged precipitation exceeds the 99th percentile of the wet-days daily precipitation intensity distribution in the climate reference (1985–2019), in at least one of the 156 WAs (Figure 1b), 94 of which are in the Northern-Italy ArCIS domain (Figure 1a). Furthermore, since some warning areas have a very small spatial extension (Figure S1), and we would like to exclude purely convective localised events that may not be associated with well-defined atmospheric patterns, similarly to Grazzini et al. (2020), we only retain events that affect an overall area covering no less than 1000 km^2. This implies we can retain some events affecting multiple–spatially connected or disconnected–small WAs, provided that the sum of their areas is equal to or greater than 1000 km^2.

2.2.2 | Characterisation of Atmospheric Circulation During EPEs

To categorise the atmospheric circulation patterns associated with EPEs over Italy, we utilise Self-Organising Maps (SOMs; Kohonen 1982), a machine learning technique popular in meteorology and climatology (e.g., Cavazos 2000; Hewitson and Crane 2002; Liu and Weisberg 2011; Sheridan and Lee 2011; Swales et al. 2016; Johnson et al. 2008; Givon et al. 2024). A SOM is an unsupervised machine learning technique used to produce a low-dimensional representation of a higher-dimensional dataset while conserving the topology and structure of the data. It usually consists of a regular two-dimensional grid of nodes arranged so that similar nodes are contiguous, while the more dissimilar ones are further apart (Sheridan and Lee 2011). The number of nodes of the SOM is a hyperparameter selected by the user depending on the specific problem at hand. In this study we test various sizes and, ultimately, we decide on a 2×2 SOM grid to classify WTs associated with EPEs over North-Central Italy, and a 3×2 grid for the whole of Italy. Additional information on the SOM validation process can be found in Appendix A. These relatively small networks generally provide a non-redundant clustering of atmospheric patterns and allow a straightforward physical interpretation of the link between the synoptic conditions and the location of EPEs. A larger SOM produces the same core patterns with additional or modified transition patterns, refining the overall structure without providing additional insight.

To identify WTs associated with EPEs, we apply SOMs to the combined daily Z500 and mSLP fields over the domain 52°N-27° N, 13°W-35° E during EPE days only. Specifically, we first compute the daily mean of each hourly variable and derive deseasonalised anomalies by subtracting a 45-day running-mean climatology. Next, for Z500 only, we remove the influence of uniform tropospheric thermal expansion by subtracting the area-weighted (weighted by the cosine of latitude) domain-mean Z500 trend (Davenport and Diffenbaugh 2021; Horton et al. 2015). Then, we standardise each field and stack the two variables to obtain combined mSLP and Z500 fields for all days with an EPE. Finally, to ensure equal-area representation in the SOM training, we weight the input data by the square root of the cosine of latitude.

We use a large spatial domain because synoptic patterns producing extreme precipitation over Italy are often related to the large-scale atmospheric circulation over the Mediterranean basin and eastern Atlantic (e.g., Miglietta and Davolio 2022). Several sensitivity experiments are conducted, changing the domain extension to shift the focus between the Atlantic and Mediterranean regions. Ultimately, we select the domain 52° N-27° N, 13° W-35° E, as it best captures the key features of the patterns without

10970088, 2025, 15, Downloaded from https://rmets.onlinelibrary.wiley.com/doi/10.1002/joc.70118 by CochraneItalia, Wiley Online Library on [03/12/2025]. See the Terms and Conditions (https://onlinelibrary.wiley.com/terms-and-conditions) on Wiley Online Library for rules of use; OA articles are governed by the applicable Creative Commons License

over-representing typical Atlantic or Mediterranean characteristics. Such a large domain extension results in the number of EPEs being much smaller than the number of spatial features (e.g., 674 events vs. 38,986 grid points for North-Central Italy). To address this issue, that could lead to computational problems, we first apply principal component analysis (PCA) in S-mode for data reduction and then run the SOM algorithm. This data preprocessing approach is commonly applied before performing clustering analysis (e.g., Federico et al. 2008; Sheridan and Lee 2011) to substantially reduce computation times and to make the clustering process more effective, reducing noise and highlighting the most relevant patterns in the data. By reducing the number of features while retaining the most informative components, we mitigate the risk of sparsity in high-dimensional spaces, which can affect the ability of the SOM to form meaningful clusters (see Appendix A for additional details).

To evaluate the robustness of the SOM algorithm in identifying coherent atmospheric patterns, we construct signal-to-noise (S2N) maps (Figure S4). These maps are generated by computing the composite anomalies of Z500 and mean sea level pressure (mSLP) for each node and dividing them by the corresponding intra-node standard deviation. Higher absolute S2N values indicate stronger agreement among the individual anomaly maps associated with a given node, thereby highlighting regions of increased pattern consistency.

Additionally, for each SOM node, we calculate composites of Z500 and mSLP and of TCWV and IVT to evaluate both the associated large-scale atmospheric dynamics and the moist thermodynamic environment. Furthermore, to determine the relevance of each WTs for EPEs in different parts of Italy, we estimate $\Phi_i(WA_j)$, that is, the percentage of EPEs in each WA associated with each WT:

$$\Phi_i(WA_j) = \frac{n_{EPE(WT_i;WA_j)}}{\sum_i n_{EPE(WT_i;WA_j)}} \quad (1)$$

where WT_i denotes the i-th WT, WA_j the j-th WA and $n_{EPE}(WT_i; WA_j)$ the number of extreme events recorded in WA_j during WT_i.

Making composites of similar patterns with slightly different positions of anomalies can lead to a "smearing" of the anomaly in the composites. To assess that, we calculate the mean pattern correlation ρ, which indicates how closely daily patterns in a SOM node match the average patterns of all days within that node.

Finally, we analyse the seasonality associated with each pattern and examine whether the frequency of precipitation extremes associated with the different WTs shows decadal variability or long-term trends. In order to assess whether the changes in the frequency of EPEs are linked to changes in the occurrence of specific WTs (dynamics) or simply to increased atmospheric moisture (thermodynamics), we investigate long-term trends in the number of days which have circulation patterns analogue to those in WTs. For a given WT, these will thus include both days associated with EPE and non-EPE days. We determine these days as those within a given "radius" in the Euclidean Distance from each SOM node (see Supportive Information for details). Statistical significance is tested using the Mann-Kendall trend test through the `pyMannKendall` package (Hussain and Mahmud 2019).

3 | Results

3.1 | Validation Over North-Central Italy

We identify WTs associated with EPEs in North-Central Italy (i.e., ArCIS domain), considering all three precipitation datasets: ArCIS, MSWEP, and CERRA. This is a necessary step to identify the best dataset to then expand the ArCIS analysis to the whole of Italy. As explained in Section 2.1, ArCIS is based on over 800 direct observations, making it a reliable precipitation dataset for North-Central Italy and a benchmark for comparison with MSWEP and CERRA.

Before examining the WTs, comparison of the 99th percentile of daily precipitation in CERRA and MSWEP to ArCIS (Figure 2) already shows that over North-Central Italy MSWEP tends to underestimate precipitation extremes, particularly in the alpine North-East, where MSWEP has large negative biases. This is probably due to insufficient daily gauge observations in the mountainous areas and/or poor calibration of satellite retrievals to match extreme precipitation values. An even larger underestimation of extremes is found in ERA5 (Figure 2d). On the other hand, CERRA shows values of the 99th percentile which are better in agreement with those of ArCIS over northern Italy.

The ability of CERRA and MSWEP to reproduce ArCIS is further assessed in terms of their performance to capture the variability in the EPEs occurring in North-Central Italy and the WTs associated with such events. Using the EPE definition from Section 2.2, we select the days within 1985 to 2019 when an EPE occurred over North-Central Italy (Figure 1a), resulting in three lists of extreme days, one for each precipitation dataset. We identify 674 EPEs for ArCIS, 813 for CERRA and 731 for MSWEP. These events overlap with those in ArCIS by 73% for CERRA and 58% for MSWEP, with correlation coefficients in the annual number of EPEs of 0.86 and 0.66, respectively (Figure S2 and Table S1).

We train a 2×2 SOM to identify the WTs of EPEs in North-Central Italy across the three precipitation datasets (Figure 3). WT1 (first column) represents a low-level anomalous cyclonic circulation located over France associated with a deep, mid-level Atlantic trough centered over northern Spain and western France. The shifted positions between the two anomalies is typical of baroclinic cyclones (Figure S3a).

WT2 (second column) is representative of a low-level cyclonic anomalous circulation over the northern Tyrrhenian Sea associated with an atmospheric trough in the upper atmosphere over north-central Europe. The analysis of mSLP (Figure S3b) reveals a typical Alpine lee cyclogenesis over the northern Tyrrhenian Sea (Bleck 1977; Buzzi et al. 2020).

The negative Z500 anomalies over northern Spain and western France and positive Z500 anomalies over eastern Europe in WT3 (Figure 3, third column, and Figure S3c) are associated with a mid-upper level atmospheric trough over France and

10970088, 2025, 15, Downloaded from https://rmets.onlinelibrary.wiley.com/doi/10.1002/joc.70118 by CochraneItalia, Wiley Online Library on [03/12/2025]. See the Terms and Conditions (https://onlinelibrary.wiley.com/terms-and-conditions) on Wiley Online Library for rules of use; OA articles are governed by the applicable Creative Commons License

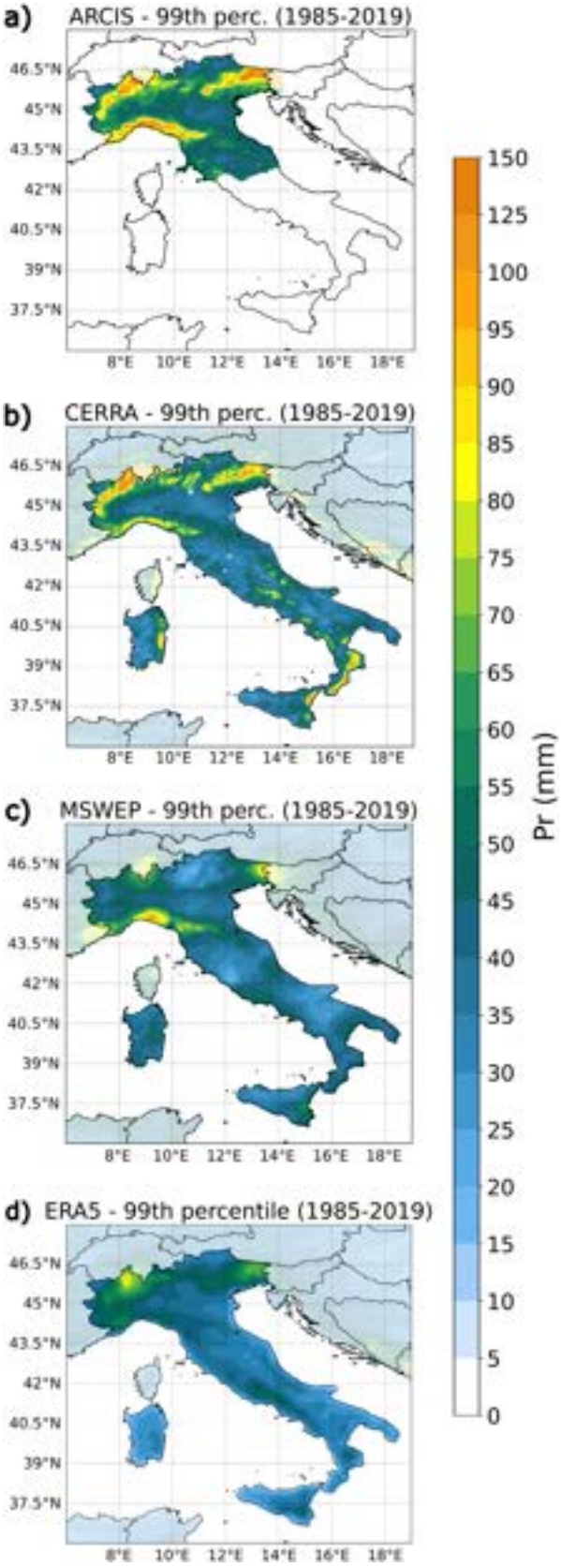

FIGURE 2 | The 99th percentile of daily precipitation computed on wet days for (a) ArCIS, (b) CERRA, (c) MSWEP precipitation datasets and (d) ERA5 reanalysis. The ERA5 99th percentile map is shown only for comparison with other products as it is not considered for estimating EPEs in this study.

northern Spain and an atmospheric ridge over central-eastern Europe. WT3 is the most recurrent (i.e., 29% of the time) during EPEs in North-Central Italy, although the relatively low mean pattern correlation ($\sim 40\% - 50\%$) suggest a certain degree of diversity of patterns during single EPEs.

Finally, the Z500 and mSLP anomalies in WT4 (fourth column) are associated with a shallow cyclonic circulation centered over the western Mediterranean Sea, located beneath an upper-level trough (Figure S3d). Z500 negative anomalies cover a wide area that goes from the Gulf of Genoa to the coasts of Algeria and Tunisia's coasts. The mSLP negative anomalies are centered over Central Italy and shifted a bit eastward in respect to the Z500 anomalies. It is the second most frequent weather type, with the second highest pattern correlation.

While WT1 and WT3 are comparable across all three datasets, overall patterns in CERRA show a better agreement with those in ArCIS. This is particularly true in the case of WT4, where MSWEP features substantial differences from ArCIS, and of WT2, with MSWEP showing an eastward-shifted anomaly. Considering that CERRA outperforms MSWEP in representing the 99th percentile of daily precipitation over Italy (Figure 2), features a higher overlap and correlation in the annual number of EPEs with ArCIS, and shows greater consistency in the SOM analysis, and assuming that the best dataset for North-Central Italy also performs best for the entire territory, we choose CERRA as the most suitable precipitation dataset to extend the EPE analysis to the entire Italian peninsula.

3.2 | Extension of Extreme Precipitation Analysis to All of Italy

Using the EPE definition (Section 2.2) based on the exceedance of the 99th daily precipitation percentile over at least 1000 km^2 for the 156 WAs across the entire peninsula (Figures 1b and 4), we identify 1534 EPEs from November 1984 to October 2024. Then, we extend the synoptic analysis developed for North-Central Italy (Section 3.1) to the whole of Italy. Given the inclusion of central-southern Italian regions which often experience heavy precipitation under different synoptic conditions from those in Northern Italy (e.g., Miglietta and Davolio 2022), a larger number of SOM nodes is required to account for the increased diversity of synoptic patterns. We choose a 2×3 SOM configuration—resulting in six different weather types (WTs)—to ensure a clear physical interpretation of the relationship between the WTs and the location of the EPEs. To test the robustness of our results, we explore a range of different SOM configurations (e.g., changing the learning rate). Apart from minor variations in the frequency and intensity of the anomalies, the patterns remain similar to those presented in the following.

Figure 5 shows the six WTs obtained by applying the SOMs to Z500 and mSLP anomalies, while Figures 6–8 show the key features of the atmospheric circulation of each WT (Section 2.2.2). Table 1 provides a summary of the main characteristics of the six WTs. The signal-to-noise map worked out for each SOM centroid (Figure S4) confirms that low-level cyclonic circulations and upper-level troughs identified by the SOM are robust, coherent features characteristic of each WT.

10970088, 2025, 15, Downloaded from https://rmets.onlinelibrary.wiley.com/doi/10.1002/joc.70118 by CochraneItalia, Wiley Online Library on [03/12/2025]. See the Terms and Conditions (https://onlinelibrary.wiley.com/terms-and-conditions) on Wiley Online Library for rules of use; OA articles are governed by the applicable Creative Commons License

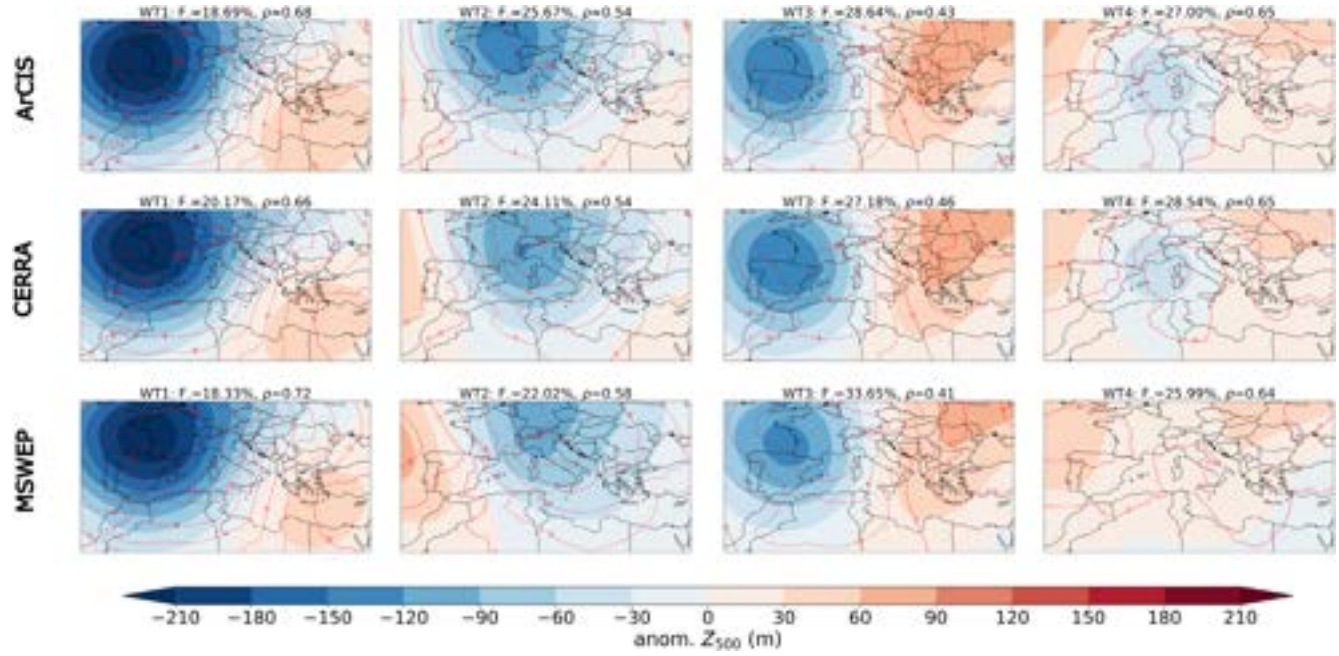

FIGURE 3 | Weather types (WTs) associated with EPEs over the ArCIS domain for the ArCIS, CERRA and MSWEP precipitation datasets (mSLP anomalies [hPa] in red contours, z500 anomalies [meters] in shading). For each WT, we present the nodal frequency (%) and the mean pattern correlation (ρ). The domain shown in each panel (52° N-27° N, 13° W-35° E) is the one used for applying SOMs.

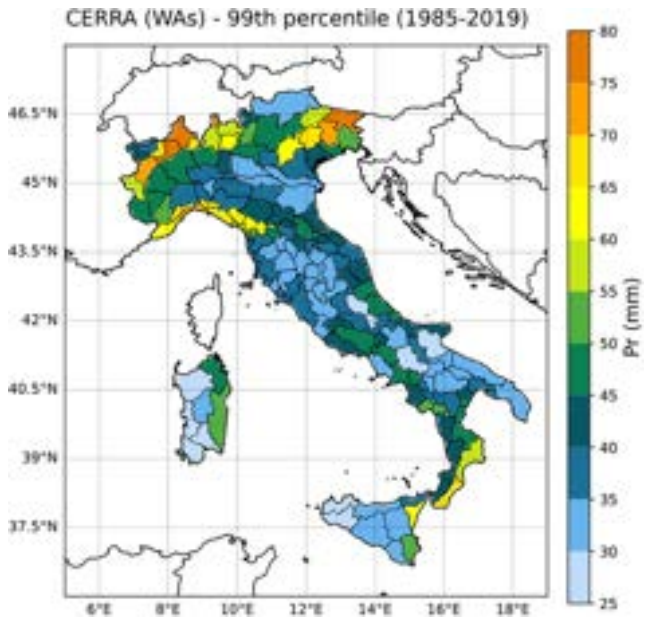

FIGURE 4 | Spatial average of the 99th percentile of daily precipitation (wet days only) across Warning Areas (WAs), based on the CERRA dataset.

WT1 is associated with a Z500 and mSLP anomaly to the west of North Italy (Figure 5a), and a strong southwesterly moisture flux over Italy (Figure 6a). It is very close to the WT1 for North-Central Italy shown in Figure 3. When looking at the Z500 and mSLP composites (Figure 6a), we note that this WT is representative of an Atlantic baroclinic cyclone located over western Europe (i.e., France) or over the northern Tyrrhenian Sea, and associated with an upper-level trough over the British Isles. As a result of the strong southerly to southwesterly IVT driven by this circulation, the Tyrrhenian side, Liguria, and Central-Eastern Alps are the Italian areas most affected by heavy precipitation events (up to 40%–50% of EPEs in some WA). WT1 is the least frequent pattern during Italian EPEs, accounting for 11.73% of all EPEs (Table 1), but it features the highest mean pattern correlation (0.75), and it is a predominantly late-autumn and winter pattern (79% of occurrences between October to February). It is less common in spring and absent in summer. Storm Vaia (also known as Adrian) (Davolio et al. 2020; Sioni et al. 2023), an intense cyclone which occurred between 27 and 30th October 2018 which affected the entire Italian peninsula and severely impacted the North Eastern Alpine region, falls within this WT.

WT2 is characterised by Z500 negative anomalies over Northwestern Italy and mSLP negative anomalies centred over Central Italy, which is indicative of a cyclonic system with a baroclinic structure (Figure 5b). The Z500 and mSLP composites (Figure 6b) reveal that this WT is consistent with a Mediterranean cyclone centred over Central Italy and associated with an upper-level trough over north-central Europe. The TCWV-IVT fields clearly indicate a cyclonic circulation, with a northwesterly IVT impacting Sardinia, a recurving southwesterly IVT impacting the southern Tyrrhenian, and a weak recurving easterly IVT advecting moisture towards the northern Adriatic coast of Italy. This circulation type explains 12.97% of all EPEs in Italy, with the most affected areas in the Eastern Po Valley and the southern Tyrrhenian side (Figure 6). While WT2 occurs throughout the year, it is most frequent in late autumn and winter. A notable event that falls within this WT is the heavy precipitation that affected Sarno (Salerno district, Campania region) on the 4th and 5th May 1998 (Esposito et al. 2023; Prete et al. 1998; Dorta et al. 2007; Mazzarella et al. 2002) and triggered a series of landslides that caused 150 casualties and considerable damage to buildings.

10970088, 2025, 15, Downloaded from https://rmets.onlinelibrary.wiley.com/doi/10.1002/joc.70118 by CochraneItalia, Wiley Online Library on [03/12/2025]. See the Terms and Conditions (https://onlinelibrary.wiley.com/terms-and-conditions) on Wiley Online Library for rules of use; OA articles are governed by the applicable Creative Commons License

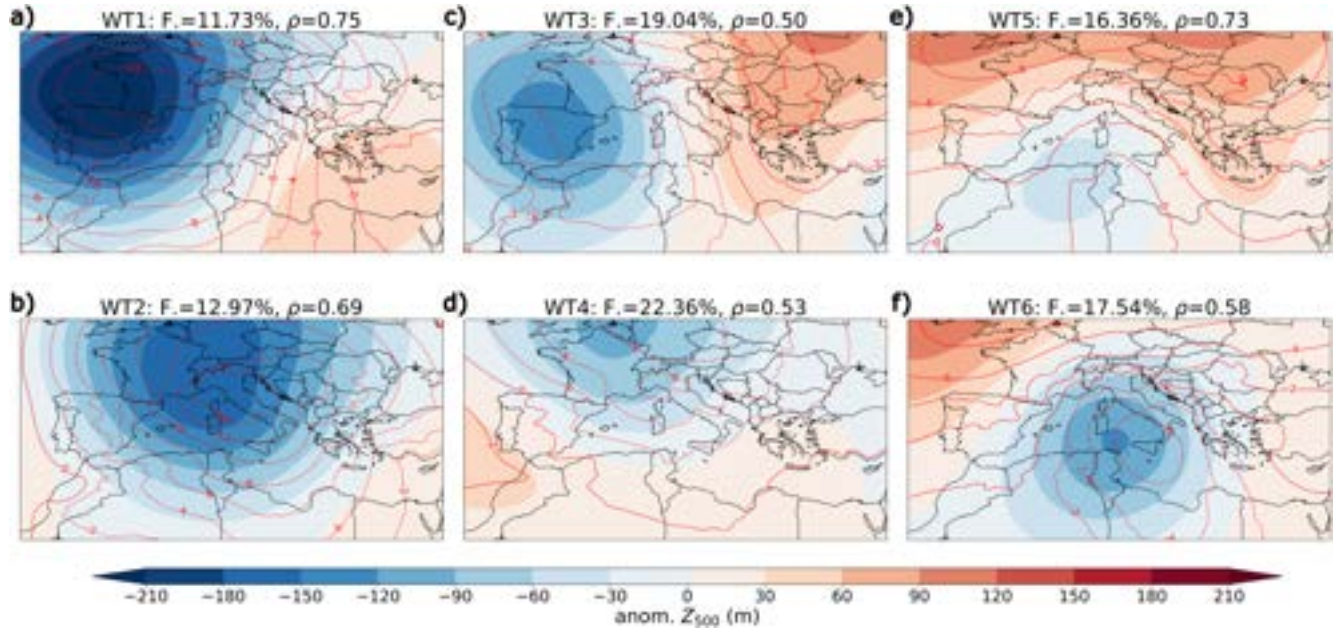

FIGURE 5 | Weather Types (mSLP anomalies [hPa] in red contours, Z500 anomalies [meters] in shading) of CERRA for all Italy. For each WT, we present the nodal frequency (%) and the mean pattern correlation (ρ). The domain shown in each panel (52° N-27° N, 13° W-35° E) is the one used for applying SOMs.

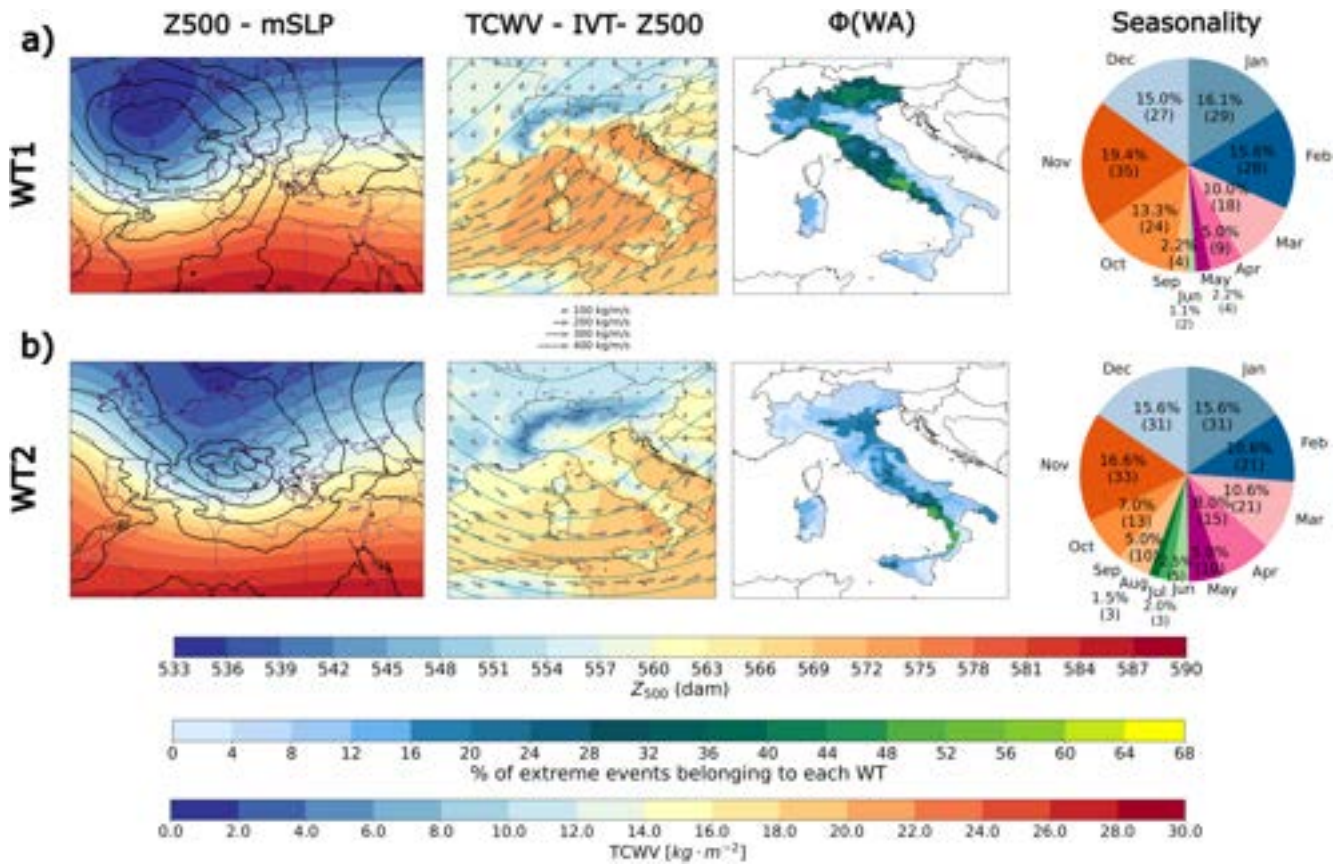

FIGURE 6 | (a) Characterisation of WT1 and (b) WT2 associated with EPEs in Italy. The first column shows composites of Z500 (shaded, in dam) and mSLP (contours, in hPa). The second column displays TCWV (shaded, in $kg\ m^{-2}$), IVT (grey arrows, in $kg\ m^{-1}\ s^{-1}$), and Z500 contours (green, in dam). The third column indicates the percentage of extreme precipitation events (EPEs) associated with each weather type. The fourth column illustrates the seasonal distribution of EPEs, with colour-coded percentages: Blue for DJF, pink for MAM, green for JJA, and orange for SON.

10970088, 2025, 15, Downloaded from https://rmets.onlinelibrary.wiley.com/doi/10.1002/joc.70118 by CochraneItalia, Wiley Online Library on [03/12/2025]. See the Terms and Conditions (https://onlinelibrary.wiley.com/terms-and-conditions) on Wiley Online Library for rules of use; OA articles are governed by the applicable Creative Commons License

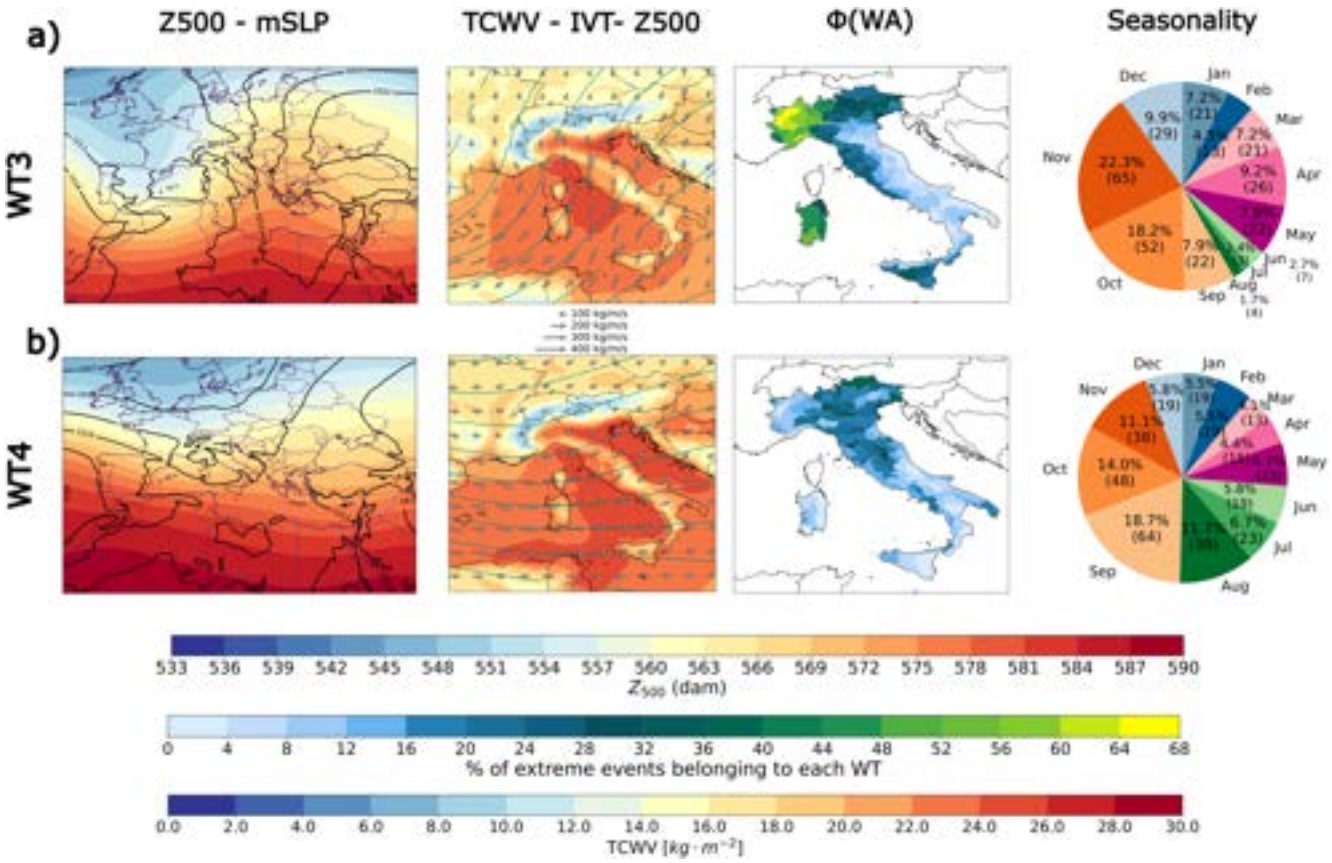

FIGURE 7 | As in Figure 6 but for (a) WT3, and (b) WT4.

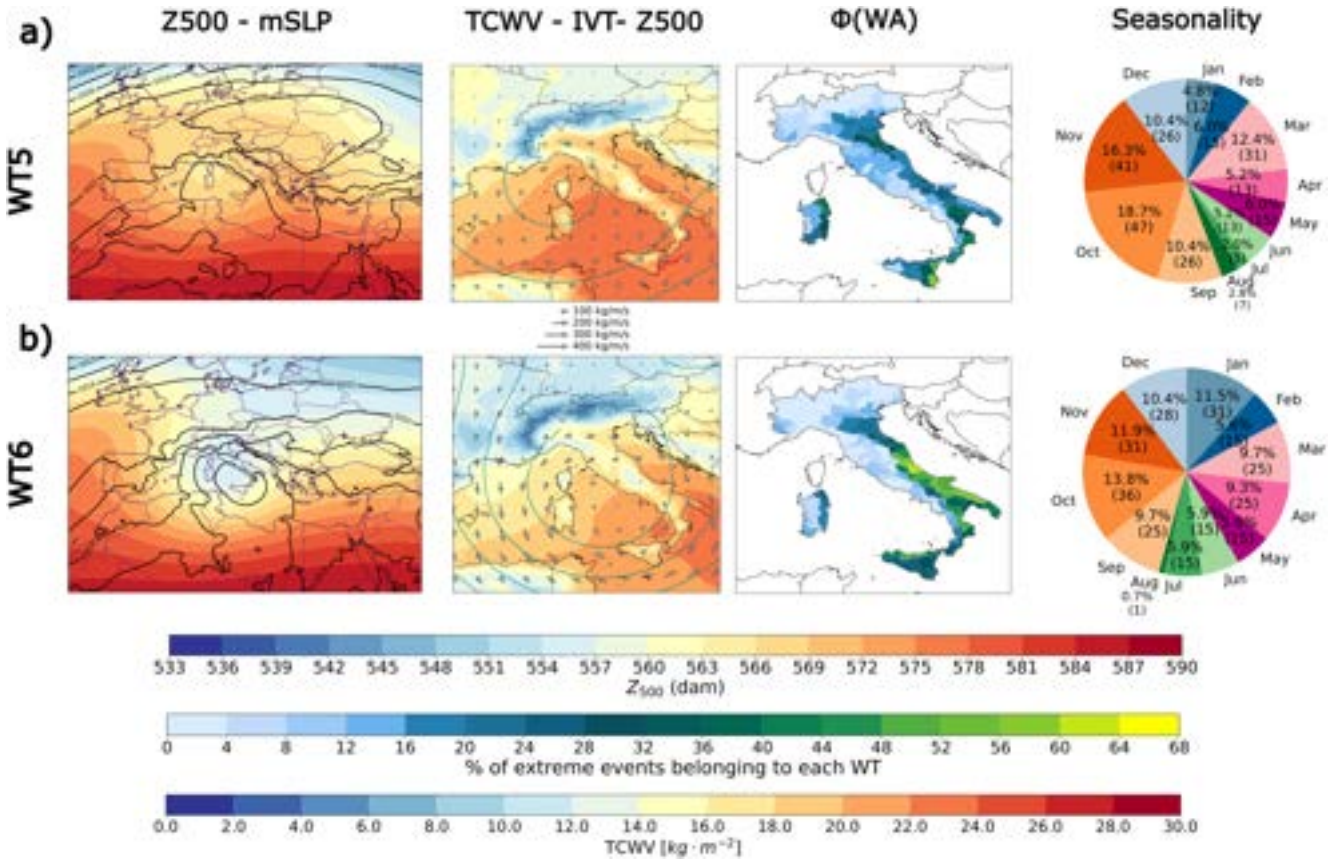

FIGURE 8 | As in Figure 6 but for (a) WT5, and (b) WT6.

10970088, 2025, 15, Downloaded from https://rmets.onlinelibrary.wiley.com/doi/10.1002/joc.70118 by CochraneItalia, Wiley Online Library on [03/12/2025]. See the Terms and Conditions (https://onlinelibrary.wiley.com/terms-and-conditions) on Wiley Online Library for rules of use; OA articles are governed by the applicable Creative Commons License

TABLE 1 | Characterisations of EPEs weather types of Italy.

	Weather type	Frequency	Moisture flux	Affected areas	Seasonality	Notable events[a]
WT1	Atlantic cyclone over France/northern Tyrrhenian Sea associated with deep upper-level trough over British Isles	11.73%	Southerly to southwesterly	Tyrrhenian side, Liguria and Central-Eastern Alps	Late Autumn, Winter, early Spring.	Storm Vaia (29-10-2018)
WT2	Mediterranean cyclone over Central Italy associated with upper-level trough over north-central Europe	12.97%	Weak cyclonic circulation (northwesterly over N. Italy, westerly over S. Italy, easterly over eastern Po Valley)	Eastern Po Valley, southern Tyrrhenian side	Autumn, Winter and Spring.	Sarno flood (04-05-1998)
WT3	Western Mediterranean cyclone associated with upper level trough over Iberia	19.04%	Southerly	Northwestern Italy, northcentral Tyrrhenian side, Eastern Alps, Sardinia, Sicily	Spring and Autumn, particularly October and November.	Major Po river flood (14-10-2000)
WT4	Westerly zonal flow associated with wide upper-level trough over north Atlantic, shallow cyclone over Ligurian Sea	22.36%	Westerly to south-westerly. High TCWV values.	North Italy, Central Alps, Tyrrhenian side	All year, particularly in Summer and Autumn.	Livorno flood (09-09-2017)
WT5	Upper-level cut off low.	16.36%	Cyclonic circulation (southerly over central and southern regions, recurving southeasterly over the Po Valley)	Adriatic Side of North-Central Italy, eastern side of Calabria, Basilicata, Sicily, and Sardinia	Spring, All year, particularly Autumn and Spring	Ionian Calabria flood (31-10-2015); Emilia Romagna Floods (02-05-2023, 19-10-2024)
WT6	Mediterranean cyclone centered over the Tyrrhenian Sea.	17.54%	Cyclonic circulation (south-westerly over S. Italy, easterly over the Po Valley)	Adriatic and Ionian side, eastern Po Valley, Sicily and eastern Sardinia	From September to July.	Romagna and Marche flood (07-10-1996); Calabria (Soverato) flood (8-9-2000); Emilia Romagna floods (16-05-2023 and 17-9-2024)

[a]In the "Notable Events" column, the dates identified as EPEs within the CERRA dataset are reported. If multiple dates associated with the same event fall under the same weather type (WT), only the day with the highest precipitation across the warning areas is indicated.

WT3 is representative of a Western Mediterranean cyclone associated with an upper level trough over Iberia (Figures 5c and 7a) and is characterised by negative Z500 anomalies centred over Spain and a mSLP minimum over the Balearic Islands. WT3 closely resembles the WT3 pattern in Figure 3, though with the Z500 negative anomalies shifted southward and a less elongated positive Z500 anomaly. The presence of an atmospheric pressure ridge over Eastern Europe (Figure 7a) produces a large pressure and geopotential height west–east gradient, which is associated with an intense southerly, moist flow over Italy and results in an elevated percentage (up to 64%) of EPEs over the exposed sides (e.g., Northwestern Italy, western Sardinia, north-central Tyrrhenian side, eastern Alps, Sicily). This is the second most common weather type associated with EPEs (19.04%) and it is most frequent in spring and autumn (particularly in October and November) and is uncommon in summer. This pattern features the lowest pattern correlation value (0.50) which is indicative of a certain degree of variability across WT cases. Falling into this category is the Piedmont flood (Cassardo et al. 2001) of October 13 to 16, 2000, which recorded over 600 mm of rainfall in 96 h and inundated large areas, causing widespread damage.

WT4 features intense westerly flow associated with a wide upper-level trough over the north Atlantic, a shallow cyclonic circulation over northern Italy and the Ligurian Sea, and a weak

10970088, 2025, 15, Downloaded from https://rmets.onlinelibrary.wiley.com/doi/10.1002/joc.70118 by CochraneItalia, Wiley Online Library on [03/12/2025]. See the Terms and Conditions (https://onlinelibrary.wiley.com/terms-and-conditions) on Wiley Online Library for rules of use; OA articles are governed by the applicable Creative Commons License

eastern European ridge (Figures 5d and 7b). It shows some similarities with WT2 of Figure 3 found for North-Central Italy. The presence of a mSLP minimum over the Ligurian Sea is likely indicative of secondary cyclogenesis (e.g., Bleck 1977; Trigo et al. 2002; Buzzi et al. 2020). Over Italy, this pattern exhibits a westerly to southwesterly IVT, featuring the highest TCWV values over the Mediterranean Sea among all weather types, with peaks over the Adriatic, the Emilia-Romagna region, and the Tyrrhenian Sea. In terms of EPE regionality, WT4 primarily affects Northern Italy and the Tyrrhenian side of Central Italy, with peaks over the north-eastern Alps, and it is the most common pattern in summer and autumn. It is the most frequent weather type in relationship to Italian EPEs (22.36%) but it features the second lowest mean pattern correlation (0.53), suggesting quite a diverse range of atmospheric patterns. The 2017 flash flood of Livorno (Arrighi and Castelli 2020; Cioni et al. 2018) falls into this category. This event occurred between the 9th and 10th of September 2017 when intense precipitation (> 100 mm in 1 h) fell in this area causing important rainfall accumulations and 9 casualties.

WT5 is representative of an upper level cut off low (Figure 8a), characterised by extensive positive Z500 and mSLP anomalies over Eastern Europe and a weak negative Z500 and mSLP anomaly over North Africa and the western Mediterranean (Figure 5e). It exhibits a cyclonic anticlockwise IVT over Italy, centred around Corsica, with high TCWV values over the Tyrrhenian Sea. As a consequence, this circulation type primarily affects the Adriatic side of North-Central Italy and the eastern side of Calabria, Basilicata, Sicily, and Sardinia. It is most common in autumn and spring. WT5 occurs with a frequency of 16.36% and features the highest mean pattern correlation (0.73), indicating a certain degree of homogeneity within this node. The Ionian Calabria flood (Avolio and Federico 2018) which occurred from 30th October to 2nd November 2015, as well as the more recent events of 1 to 3 May 2023 (ARPAE 2023b; Dorrington, Wenta, et al. 2024; Arrighi and Domeneghetti 2024; Cremonini et al. 2024), which heavily affected several cities in the Emilia-Romagna region (notably Forlì-Cesena, Ravenna, Rimini, and Bologna), and the 19 to 20 October 2024 flood (ARPAE 2024c), which had a particularly intense impact on the city of Bologna, fall within this WT.

Finally, WT6 represents a Mediterranean cyclone centred over the Tyrrhenian Sea (Figure 8b, see also Figure 5f for anomalies). It is the third most frequent pattern (17.54%) during Italian EPEs with a relatively low pattern correlation (0.58). Compared to WT5, WT6 exhibits higher IVT values, with south-westerly orientation over Southern Italy and easterly over the Po Valley. Additionally, the high TCWV values are displaced eastward, towards the Adriatic and Ionian Seas. The Adriatic and Ionian side, the eastern Po Valley and the extreme south of Italy are particularly exposed to heavy precipitation events when this weather pattern occurs. It is the second most common pattern in summer, and also occurs frequently in autumn and spring. Within this category, we identify four extreme events with significant impacts: the Romagna and Marche flood, which occurred between October 7 and 9, 1996, caused by Medicane Cornelia (Mazza et al. 2017), the Soverato flood (Montani et al. 2003) of September 10, 2000, which led to 13 casualties and the Emilia Romagna floods of 16 to 18 May 2023 (Dorrington, Wenta, et al. 2024; Arrighi and Domeneghetti 2024; ARPAE 2023a), which affected a wide portion of the region including Bologna, Forl-Cesena, Ravenna, and Rimini, and—together with the earlier event of 1 to 3 May of the same year—resulted in a total of 17 fatalities; and of 17 to 19 September 2024 (ARPAE 2024a; Ferrari et al. 2025), which was particularly severe in the Lamone River basin and surrounding areas.

3.2.1 | Trend Analysis

We first examine whether the annual number of EPEs has significantly changed over the study period, regardless of their associated WTs. Figure 9 shows that the overall number of EPEs has been increasing over the period 1985–2023, with a statistically significant trend (p value = 0.01) of approximately 2 EPEs per year per decade. Next, we assess whether the occurrence of EPEs linked to specific WTs has significantly changed. Figure 10 shows that the annual frequency of these EPEs is increasing in 5 out of the 6 WTs, although trends are statistically significant (p value < 0.05) only for WT4, which exhibits an increasing trend. A seasonal breakdown of the analysis for WT4 reveals no significant statistical trends, thus implying the annual mean signal is not dominated by any specific season (Figure S5). On the other hand, a strong seasonal positive trend is found for WT6 during March–May (p value = 0.03, Figure S6).

The fact that a positive trend is common to most WTs—although not statistically significant—suggests that the signal is primarily thermodynamic in nature. As a verification, we examine whether there are changes in the frequency of days with atmospheric circulation patterns analogue to the identified WTs (see Supportive Information), but we do not find any significant trends (Figures S7 and S8).

4 | Discussion

Most of the WTs identified are characterised by low-level cyclonic circulation associated with a westward displaced upper-level trough, a configuration typical of the growing phase of midlatitude baroclinic cyclones (e.g., Holton and Hakim 2013). Trigo et al. (2002) highlight how winter cyclogenesis with significant impacts on the northern Mediterranean is driven by upper-level synoptic troughs, while, in spring and summer, cyclogenesis is additionally influenced by land-sea thermal contrast too. In our classification, patterns with deep atmospheric troughs (WT1, WT2) have a strong winter component and are nearly absent in summer, whereas those linked to land cyclogenesis (WT4, WT5, WT6) exhibit a pronounced spring–summer component. Among these, the first, WT4, the most frequent pattern overall, and the latter, WT6, occur in spring and summer in almost 40% of the occurrences.

Our results are in good agreement with those of Grazzini et al. (2020) as far as North-Central Italy is concerned. Specifically, WT2, WT3, and WT4 identified here resemble the weather types Cat1, Cat2, and Cat3 of Grazzini et al. (2020). Minor differences—such as a more pronounced trough in Cat1 and a broader mSLP minimum in Cat3—are likely to be due to the different study periods (1979–2015 vs. 1984–2024) and the use of different methodologies.

10970088, 2025, 15, Downloaded from https://rmets.onlinelibrary.wiley.com/doi/10.1002/joc.70118 by CochraneItalia, Wiley Online Library on [03/12/2025]. See the Terms and Conditions (https://onlinelibrary.wiley.com/terms-and-conditions) on Wiley Online Library for rules of use; OA articles are governed by the applicable Creative Commons License

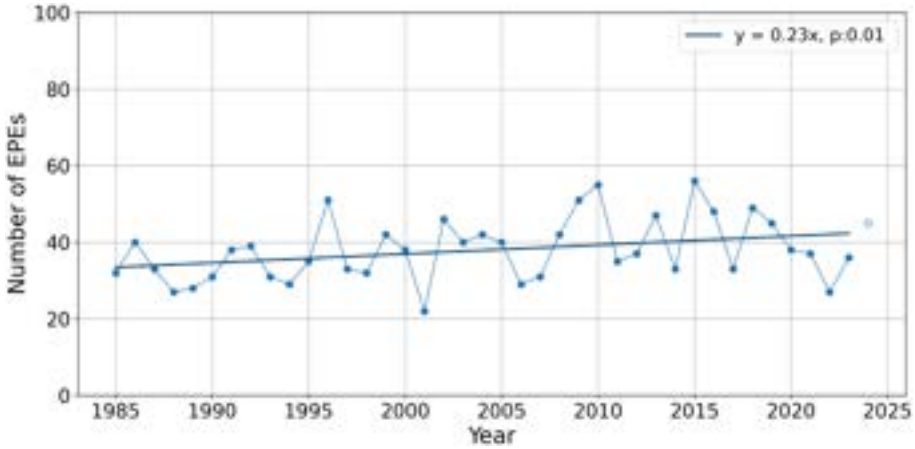

FIGURE 9 | Annual number of EPEs associated with all weather types (WTs). The trend line, calculated using only complete years (1985–2023), is shown in dark blue. Data for 1984 are excluded, while 2024 is represented by a hollow circle to indicate that the year is incomplete. The significance of the trend was assessed using the Mann-Kendall test, revealing a statistically significant increase in the occurrence of EPEs associated with WTs ($p < 0.05$).

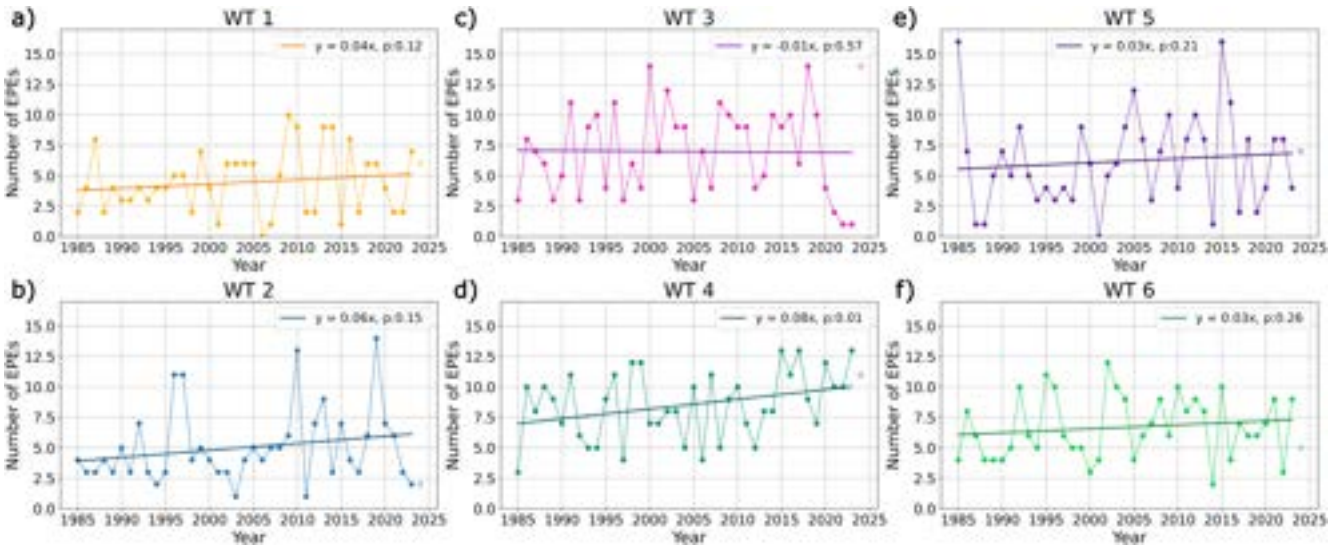

FIGURE 10 | Annual number of EPEs associated with (a) WT1, (b) WT2, (c) WT3, (d) WT4, (e) WT5, and (f) WT6. Trend lines, computed using only complete years (1985–2023), are overlaid in each panel. Data for 1984 are excluded, while 2024 is shown as a hollow circle to indicate that the year is incomplete. Trend significance was assessed using the Mann-Kendall test; only WT4 exhibits a statistically significant trend ($p < 0.05$).

We also find similarities with some of the cyclonic circulations identified by Iannuccilli et al. (2021), although a direct comparison with our study is difficult due to substantial methodological differences. In fact, Iannuccilli et al. (2021) consider all days for their classification and use a fairly small spatial domain around Italy, whereas our study focuses only on extreme precipitation days and uses a larger Euro-Mediterranean domain to represent weather types. In particular, their Circulation Type 6 (CT6) is similar to our WT4 and their CT9 to our WT6. In contrast, the seasonal distribution differs, as CT6 and CT9 have a strong winter component, whereas WT4 occurs predominantly in summer and WT6 displays a weaker or less consistent seasonal pattern. However, Iannuccilli et al. (2021) report higher EF values (the Effectiveness index in Iannuccilli et al. (2021) measures how representative a circulation pattern is of extreme days) in summer than in winter for both patterns. This suggests that, despite CT6 and CT9 being most frequent in winter, they are actually more representative of extreme precipitation events in summer. This difference may be attributed to the fact that Iannuccilli et al. (2021) include all days in their classification, rather than restricting their analysis to extreme ones. CT2 is another cyclonic circulation that affects the eastern side of Italy, and the most comparable pattern on our side appears to be WT2. Both display an mSLP minimum over Italy. However, WT2 features a well-defined closed minimum, whereas CT2 shows a broader one. Due to the limited domain of CT2, it is unclear whether this minimum is fully closed.

Capozzi et al. (2023) identify six weather types relevant for heavy precipitation over the Campania region, with five of these patterns associated with atmospheric troughs over North-Central Italy (with different intensity and shape) and a mSLP minimum over North-Central Italy. The sixth pattern is

10970088, 2025, 15, Downloaded from https://rmets.onlinelibrary.wiley.com/doi/10.1002/joc.70118 by CochraneItalia, Wiley Online Library on [03/12/2025]. See the Terms and Conditions (https://onlinelibrary.wiley.com/terms-and-conditions) on Wiley Online Library for rules of use; OA articles are governed by the applicable Creative Commons License

characterised by a zonal flow with an mSLP minimum over the Tyrrhenian Sea. Our results compare relatively well with those of Capozzi et al. (2023), with WT1 and WT2—the most relevant for the Campania region—closely resembling their circulation patterns. Federico et al. (2008) identify that atmospheric troughs or cut-off lows positioned over Central-Southern Italy typically produce intense precipitation on the southeastern/Ionian side of Calabria, while cut-off lows over the Iberian Peninsula or France primarily lead to orographic precipitation on the Tyrrhenian side. Additionally, deep atmospheric troughs over central Europe are associated with heavy precipitation on the northwestern side of Calabria. Similar patterns can be recognised in WT2, WT3, WT5, and WT6, all affecting Calabria.

Finally, Mastrantonas et al. (2021) identify nine atmospheric circulation patterns associated with extreme precipitation events (EPEs) in the Mediterranean Basin, using ERA5 reanalysis data over the period 1979 to 2019 and considering all days. Their Cl2 (Biscay Low), Cl3 (Iberian Low), and Cl4 (Sicilian Low) closely resemble our WT1, WT3, and WT5, respectively. In addition, Cl5 (Balcan Low) also appears similar to WT2, although with slightly shifted anomaly patterns. Our results are in agreement with those presented in Mastrantonas et al. (2022), where the aforementioned atmospheric circulation patterns are linked with EPEs over Calabria. Specifically, when negative anomalies are located north of Calabria (WT1, WT2, WT4), the western parts of the region are affected by heavy precipitation, while when they are located south or further west towards the Iberian Peninsula (WT3, WT5, WT6), the most impacted are the eastern and southern warning areas.

The trend analysis performed using CERRA over the period 1985–2023 on the frequency of EPEs has already identified a general upward trend. In particular, an increase of about 2 EPEs per year per decade has been observed (Figure 9). Specifically, five out of six WTs show that the annual number of these events is increasing. Moreover, we found no increase in the occurrence of the days with atmospheric circulation patterns analogue to the identified WTs, which supports the hypothesis that the observed trend in Italian EPEs is mainly driven by thermodynamic factors. Between all patterns, only WT4, the westerly zonal flow associated with a wide upper-level trough over the north Atlantic, shows a statistically significant trend with a p value of 0.01 (Figure 10). However, a loss of statistical significance is expected when analysing disaggregated data, as the associated noise tends to increase with disaggregation.

It is worth noting that WT3, the only regime for which EPE frequency does not increase, also shows the largest decrease in the frequency of analogue days (Figure S8). This suggests that variability or changes in atmospheric circulation might still play a role in modulating the relative contribution of different WTs to EPEs in the future.

Considering the seasonal decomposition in the EPE trend analysis, no statistically significant trends are identified overall, primarily due to increased disaggregation and the resulting higher noise. For instance, WT4, which shows a significant positive trend in the annual frequency, does not show any trends in the seasonal decomposition, meaning that the increase of this pattern is not driven by a rise in occurrences during a specific season. An exception is observed for WT6, the Mediterranean Cyclone, which exhibits a statistically significant increasing trend during the MAM season.

It is worth highlighting that this category includes the second phase of the May 2023 flood that struck Emilia-Romagna between the 15th and 17th of May, which led to a total of 16 casualties (including the first phase) and €9 billion of damages (AST 2023). In this context, our results align with the findings of Dorrington, Wenta, et al. (2024), who showed that the Emilia-Romagna floods of May 2023—particularly the second phase—were associated with an anomalously high water vapour flux from the eastern quadrants that the Mediterranean Cyclones with a similar configuration to WT6 appear to be related to the gradient of temperature over the Mediterranean basin. As the north–south gradient between North Africa and the Mediterranean strengthens, precipitation along the Adriatic side tends to increase. However, further analysis may be required to confirm this hypothesis.

5 | Conclusions

In this study, we show that a regional reanalysis dataset (CERRA) outperforms a state-of-the-art global satellite-based dataset (MSWEP) in representing precipitation extremes in Italy, showing overall satisfactory skill against a high-quality gauge-based dataset (ArCIS). The use of the CERRA reanalysis dataset enables us to establish a general framework for studying precipitation extremes in Italy, which suffers from the lack of nationwide quality-controlled and homogenised precipitation datasets.

Using self-organising maps, we classify weather types linked to precipitation extremes in the period November 1984 to October 2024, and link them to large-scale atmospheric circulation patterns over Europe and the eastern North Atlantic. This work builds upon several recent studies that investigated the atmospheric circulation drivers of heavy precipitation events over the Italian peninsula (e.g., Miglietta and Davolio 2022; Sioni et al. 2023; Grazzini et al. 2020; Iannuccilli et al. 2021; Capozzi et al. 2023; Federico et al. 2008; Mastrantonas et al. 2021, 2022). However, some of the aforementioned studies either relied on individual, scattered weather stations (e.g., Iannuccilli et al. 2021) or had a very regional focus (e.g., Capozzi et al. 2023; Federico et al. 2008; Mastrantonas et al. 2022). Our research extends previous work by presenting a more comprehensive classification of the large-scale weather patterns that drive heavy precipitation throughout Italy. In summary, our results corroborate previous research and, in addition, provide a comprehensive large-scale classification of circulation patterns associated with EPEs across Italy. The identified WTs exhibit well-defined dynamics, and our methodology allows us to recognise the most impactful pattern for any chosen area. Moreover, many notable events that occurred in the northern and southern regions have been related to our WTs. A possible caveat is that CERRA has been validated against an observational dataset (ArCIS) only in the centre-north of Italy. That the dataset has a similar accuracy also in the south of Italy is a plausible, but untested, assumption. Nevertheless, our method is highly adaptable and can be applied

10970088, 2025, 15, Downloaded from https://rmets.onlinelibrary.wiley.com/doi/10.1002/joc.70118 by CochraneItalia, Wiley Online Library on [03/12/2025]. See the Terms and Conditions (https://onlinelibrary.wiley.com/terms-and-conditions) on Wiley Online Library for rules of use; OA articles are governed by the applicable Creative Commons License

to any high-resolution precipitation datasets covering the whole of Italy.

A key question to address in the context of climate change is whether the increase in EPEs frequency, observed in CERRA (2 EPEs/year per decade, Mann–Kendall, p value <0.05), will translate into a uniform increase across all weather types (WTs), or whether specific patterns will be more substantially affected. This has crucial implications, as spatially heterogeneous responses among WTs would lead to varying degrees of exposure and vulnerability across different regions. The trend analysis performed over the period from 1985 to 2023 shows that only one pattern (WT4) exhibits a significant positive trend in the annual frequency. A possible interpretation for a positive trend in WT4 is that either westerly zonal flow associated with an upper-level trough over the north Atlantic has become more frequent in recent years or that their ability to trigger an Italian precipitation extreme, despite on average weaker circulation anomalies in respect of the other identified patterns, has increased. This can be induced by an enhanced moisture availability from a warmer Mediterranean Sea. Since the overall occurrence of days with a similar Z500 and SLP anomaly to WT4 (considering all days, including those with no precipitation) has not increased, a more plausible explanation is that, under current global warming conditions, even synoptic anomalies which had a non-extreme precipitation impact at the beginning of the climatological period can now lead to EPEs. This is likely due to increased atmospheric moisture content, which enhances the potential for EPEs in association with WT4-like circulation.

Identifying the causes of this trend and understanding the time of emergence for future changes is beyond the scope of this study and would require the use of large ensemble climate model simulations in order to isolate the contributions of natural variability and human-caused climate change (Otto 2017; National Academies of Sciences, Engineering, and Medicine 2016; Deser et al. 2020). Recent studies show that the combined use of machine-learning approaches and large ensembles of climate model simulations has been successfully applied for assessing the influence of anthropogenic climate change on atmospheric circulation patterns associated with specific extreme meteoclimatic events (e.g., Harrington et al. 2016; Odoulami et al. 2023; Mittermeier et al. 2019). When combined with a classification method (e.g., Davenport and Diffenbaugh 2021), these results offer a framework applicable to climate model simulations, enabling the assessment of climate change impacts on the drivers of precipitation extremes over Italy. This will be the focus of future work, where we plan to employ deep learning techniques to estimate the conditional probability of extreme precipitation events for each weather type.

Author Contributions

Cristina Iacomino: writing – original draft, investigation, software, formal analysis, methodology, visualization. **Salvatore Pascale:** conceptualization, funding acquisition, investigation, supervision, writing – review and editing. **Giuseppe Zappa:** conceptualization, funding acquisition, data curation, project administration, writing – review and editing. **Marcello Iotti:** writing – review and editing, data curation. **Federico Grazzini:** writing – review and editing, resources. **Paolo Ghinassi:** writing – review and editing. **Alice Portal:** writing – review and editing.

Acknowledgements

This research was carried out under the ENCIRCLE ("Evaluating the changing risk of cyclones for Italian precipitation extremes") project, funded by the European Union—Next Generation EU, Mission 4, Component 1, CUP B53D23006830006. The authors would like to acknowledge the Italian Department of Civil Protection for providing the shape files of the warning area units, and Claudia Simolo for the useful discussions. We acknowledge the tutorial of Kurtz and Martin (2023) on the Python package MiniSom as a starting point for our coding. Finally, we gratefully acknowledge the two anonymous reviewers for their constructive comments and suggestions, which helped improve the quality of this manuscript. Open access publishing facilitated by Universita degli Studi di Bologna, as part of the Wiley - CRUI-CARE agreement.

Conflicts of Interest

The authors declare no conflicts of interest.

Data Availability Statement

The ArCIS precipitation dataset is available online at https://www.arcis.it/wp/prodotti/. The MSWEP precipitation product can be requested online at https://www.gloh2o.org/mswep/. CERRA was downloaded from the Copernicus Climate Change Service (2021), ERA5 was downloaded from the Copernicus Climate Change Service (2023a) and the Copernicus Climate Change Service (2023b). The results contain modified Copernicus Climate Change Service information 2020. Neither the European Commission nor ECMWF is responsible for any use that may be made of the Copernicus information or data it contains. The code used for the SOM classification is available at https://github.com/ciacomin/ENCIRCLE-MiniSom.

References

AEMET Agencia Estatal de Meteorología. 2024. *Estudio sobre la situación de lluvias intensas, localmente torrenciales y persistentes, en la Peninsula Ibérica y Baleares entre los das 28 de octubre y 4 de noviembre de 2024*. AEMET Agencia Estatal de Meteorología. Technical report. https://www.aemet.es/es/conocermas/recursos_en_linea/publicaciones_y_estudios/estudios/detalles/dana_oct_24_prelim.

Allen, M. R., and W. J. Ingram. 2002. "Constraints on Future Changes in Climate and Thehydrological Cycle." *Nature* 419: 224–232. https://doi.org/10.1038/nature01092.

Antolini, G., L. Auteri, V. Pavan, F. Tomei, R. Tomozeiu, and V. Marletto. 2016. "A Daily High-Resolution Gridded Climatic Data Set for Emilia-Romagna, Italy, During 1961–2010." *International Journal of Climatology* 36, no. 4: 1970–1986. https://doi.org/10.1002/joc.4473.

ARPAE. 2023a. "*Rapporto degli eventi meteorologici di piena e di frana del 16-18 maggio 2023*. ARPAE Emilia-Romagna, Technical report." https://www.arpae.it/it/notizie/rapporto_idro_meteo_20230516-18.pdf.

ARPAE. 2023b. "*Rapporto degli eventi meteorologici di piena e di frana dell'1–4 maggio 2023*. ARPAE Emilia-Romagna, Technical report." https://www.arpae.it/it/notizie/rapporto_meteo_20230501-04.pdf.

ARPAE. 2024a. "*Analisi speditiva dell'evento del 17–19 settembre 2024 sulla regione Emilia-Romagna*. Preliminary Report conducted by Regional Functional Center ARPAE-SIMC, in collaboration with the Geology, Soils, and Seismic Area of the Emilia-Romagna Region." https://www.arpae.it/it/notizie/alluvione-19-settembre-un2019analisi-preliminare.

10970088, 2025, 15, Downloaded from https://rmets.onlinelibrary.wiley.com/doi/10.1002/joc.70118 by CochraneItalia, Wiley Online Library on [03/12/2025]. See the Terms and Conditions (https://onlinelibrary.wiley.com/terms-and-conditions) on Wiley Online Library for rules of use; OA articles are governed by the applicable Creative Commons License

ARPAE. 2024b. "Maltempo, *oltre 350 millimetri di pioggia caduta*. ARPAE Emilia-Romagna." https://www.arpae.it/it/notizie/maltempo-oltre-350-millimetri-di-pioggia-caduta.

ARPAE. 2024c. "Primi dati sulle precipitazioni del 19 ottobre. ARPAE Emilia-Romagna." https://www.arpae.it/it/notizie/primi-dati-sulle-precipitazioni-del-19-ottobre.

Arrighi, C., and F. Castelli. 2020. "The 2017 Flash Flood of Livorno (Italy): Lessons Learnt From an Exceptional Hydrologic Event." In *Advances in Natural Hazards and Hydrological Risks: Meeting the Challenge*, edited by F. Fernandes, A. Malheiro, and H. I. Chaminé, 117–120. Springer International Publishing. https://doi.org/10.1007/978-3-030-34397-2_23.

Arrighi, C., and A. Domeneghetti. 2024. "Brief Communication: On the Environmental Impacts of the 2023 Floods in Emilia-Romagna (Italy)." *Natural Hazards and Earth System Sciences* 24: 673–679. https://doi.org/10.5194/nhess-24-673-2024.

AST. 2023. "*Alluvione. oltre 8,8 miliardi di euro: è la stima provvisoria dei danni, di cui 1,8 per interventi necessari a fare fronte all'emergenza*. Agenzia per la Sicurezza Territoriale e la Protezione Civile Emilia-Romagna." https://protezionecivile.regione.emilia-romagna.it/notizie/2023/giugno/alluvione-oltre-8-8-miliardi-di-euro-la-stima-provvisoria-dei-danni-di-cui-1-8-per-interventi-necessari-a-fare-fronte-emergenza.

Avolio, E., and S. Federico. 2018. "WRF Simulations for a Heavy Rainfall Event in Southern Italy: Verification and Sensitivity Tests." *Atmospheric Research* 209: 14–35. https://www.sciencedirect.com/science/article/pii/S016980951731075X.

Ban, N., J. Rajczak, J. Schmidli, and C. Schär. 2020. "Analysis of Alpine Precipitation Extremes Using Generalized Extreme Value Theory in Convection-Resolving Climate Simulations." *Climate Dynamics* 55, no. 1: 61–75. https://doi.org/10.1007/s00382-018-4339-4.

Bandhauer, M., F. Isotta, M. Lakatos, et al. 2022. "Evaluation of Daily Precipitation Analyses in e-Obs (v19.0e) and era5 by Comparison to Regional High-Resolution Datasets in European Regions." *International Journal of Climatology* 42, no. 2: 727–747. https://doi.org/10.1002/joc.7269.

Beck, C., and A. Philipp. 2010. "Evaluation and Comparison of Circulation Type Classifications for the European Domain." *Physics and Chemistry of the Earth* 35: 374–387. https://doi.org/10.1016/j.pce.2010.01.001.

Beck, H., and National Center for Atmospheric Research Staff. 2023. "*The Climate Data Guide: Global High-Resolution Precipitation: Mswep.*" https://climatedataguide.ucar.edu/climate-data/global-high-resolution-precipitation-mswep.

Bellman, R. 1961. *Adaptive Control Processes: A Guided Tour*. Princeton University Press. https://doi.org/10.1515/9781400874668.

Bellman, R. 1984. *Dynamic Programming*. Princeton University Press.

Bleck, R. 1977. "Numerical Simulation of Lee Cyclogenesis in the Gulf of Genoa." *Monthly Weather Review* 105: 428–445. https://doi.org/10.1175/1520-0493(1977)105%3C0428:NSOLCI%3E2.0.CO;2.

Buzzi, A., S. Davolio, and M. Fantini. 2020. "Cyclogenesis in the Lee of the Alps: A Review of Theories." *Bulletin of Atmospheric Science and Technology* 1, no. 3: 433–457. https://doi.org/10.1007/s42865-020-00021-6.

Capozzi, V., C. Annella, and G. Budillon. 2023. "Classification of Daily Heavy Precipitation Patterns and Associated Synoptic Types in the Campania Region (Southern Italy)." *Atmospheric Research* 289: 106781. https://doi.org/10.1016/j.atmosres.2023.106781.

Casado, M., and M. Pastor. 2016. "Circulation Types and Winter Precipitation in Spain." *International Journal of Climatology* 36: 2727–2742. https://doi.org/10.1002/joc.3860.

Cassardo, C., R. Cremonini, D. Gandini, G. Paesano, R. Pelosini, and M. W. Qian. 2001. "Analysis of the severe flood of 13t-16th October 2000 in Piedmont (Italy). *Cuadernos de investigación geográfica, ISSN 0211–6820, Nº 27, 2001, pags. 147–162*, 27." https://doi.org/10.18172/cig.1120.

Cavalleri, F., C. Lussana, F. Viterbo, et al. 2024. "Multi-Scale Assessment of High-Resolution Reanalysis Precipitation Fields Over Italy." *Atmospheric Research* 312: 107734. https://doi.org/10.1016/j.atmosres.2024.107734. https://www.sciencedirect.com/science/article/pii/S0169809524005167.

Cavazos, T. 2000. "Using Self-Organizing Maps to Investigate Extreme Climate Events: An Application to Wintertime Precipitation in the Balkans." *Journal of Climate* 13, no. 10: 1718–1732. https://doi.org/10.1175/1520-0442(2000)013%3C1718:USOMTI%3E2.0.CO;2.

CBS News. 2024. "*Spain Floods Death Toll Hits 205 as Maps, Satellite Images Reveal Valencia Impact and Residents Blast Response*." https://www.cbsnews.com/news/spain-floods-deaths-maps-satellite-images-valencia-impact-resident-anger-response/.

Cioni, G., D. Cerrai, A. Ricchi, et al. 2018. "A numerical study of the livorno 9-10 september 2017 flash floodIn: Geophysical Research Abstracts. 20." EGU2018-19253. Presented at: EGU General Assembly 2018.

Copernicus Climate Change Service, C.D.S. 2021. "Cerra sub-daily regional reanalysis data for europe on single levels from 1984 to present." https://doi.org/10.24381/cds.622a565a.

Copernicus Climate Change Service, C.D.S. 2023a. "Era5 hourly data on pressure levels from 1940 to present." https://doi.org/10.24381/cds.bd0915c6.

Copernicus Climate Change Service, C.D.S. 2023b. "Era5 hourly data on single levels from 1940 to present." https://doi.org/10.24381/cds.adbb2d47.

Cremonini, L., P. Randi, M. Fazzini, M. Nardino, F. Rossi, and T. Georgiadis. 2024. "Causes and Impacts of Flood Events in Emilia-Romagna (Italy) in May 2023." *Land* 13, no. 11: 1800. https://doi.org/10.3390/land13111800.

Da Silva, N. A., and J. O. Haerter. 2025. "Super-Clausius–Clapeyron Scaling of Extreme Precipitation Explained by Shift From Stratiform to Convective Rain Type." *Nature Geoscience* 18, no. 5: 382–388. https://doi.org/10.1038/s41561-025-01686-4.

Davenport, F. V., and N. S. Diffenbaugh. 2021. "Using Machine Learning to Analyze Physical Causes of Climate Change: A Case Study of U.S. Midwest Extreme Precipitation." *Geophysical Research Letters* 48, no. 15: e2021GL093787. https://doi.org/10.1029/2021GL093787.

Davolio, S., S. D. Fera, S. Laviola, M. M. Miglietta, and V. Levizzani. 2020. "Heavy Precipitation Over Italy From the Mediterranean Storm "Vaia" in October 2018: Assessing the Role of an Atmospheric River." *Monthly Weather Review* 148, no. 9: 3571–3588. https://doi.org/10.1175/MWR-D-20-0021.1.

Deser, C., F. Lehner, K. B. Rodgers, et al. 2020. "Insights From Earth System Model Initial-Condition Large Ensembles and Future Prospects." *Nature Climate Change* 10: 277–286. https://doi.org/10.1038/s41558-020-0731-2.

Dorrington, J., C. Grams, F. Grazzini, L. Magnusson, and L. Vitart. 2024. "Domino: A New Framework for the Automated Identification of Weather Event Precursors, Demonstrated for European Extreme Rainfall." *Quarterly Journal of the Royal Meteorological Society* 150, no. 759: 776–795. https://doi.org/10.1002/qj.4622.

Dorrington, J., M. Wenta, F. Grazzini, L. Magnusson, F. Vitart, and C. M. Grams. 2024. "Precursors and Pathways: Dynamically Informed Extreme Event Forecasting Demonstrated on the Historic Emilia-Romagna 2023 Flood." *Natural Hazards and Earth System Sciences* 24: 2995–3012. https://doi.org/10.5194/nhess-24-2995-2024.

Dorta, D. O., G. Toyos, C. Oppenheimer, M. T. Pareschi, R. Sulpizio, and G. Zanchetta. 2007. "Empirical Modelling of the May 1998 Small Debris Flows in Sarno (Italy) Using LAHARZ." *Natural Hazards* 40, no. 2: 381–396. https://doi.org/10.1007/s11069-006-0035-5.

10970088, 2025, 15, Downloaded from https://rmets.onlinelibrary.wiley.com/doi/10.1002/joc.70118 by CochraneItalia, Wiley Online Library on [03/12/2025]. See the Terms and Conditions (https://onlinelibrary.wiley.com/terms-and-conditions) on Wiley Online Library for rules of use; OA articles are governed by the applicable Creative Commons License

ECMWF. 2024. "*Storm Boris and European Flooding in September 2024*." https://www.ecmwf.int/en/about/media-centre/focus/2024/storm-boris-and-european-flooding-september-2024.

Esposito, G., P. Salvati, and C. Bianchi. 2023. "Insights Gained Into Geo-Hydrological Disaster Management 25 Years After the Catastrophic Landslides of 1998 in Southern Italy." *International Journal of Disaster Risk Reduction* 84: 103440. https://doi.org/10.1016/j.ijdrr.2022.103440.

Federico, S., E. Avolio, L. Pasqualoni, and C. Bellecci. 2008. "Atmospheric Patterns for Heavy Rain Events in Calabria." *Natural Hazards and Earth System Sciences* 8, no. 5: 1173–1186. https://doi.org/10.5194/nhess-8-1173-2008.

Ferrari, A., G. Passadore, R. Vacondio, et al. 2025. "Brief Communication: Hydrological and Hydraulic Investigation of the Extreme September 2024 Flood on the Lamone River in Emilia-Romagna, Italy." *Natural Hazards and Earth System Sciences* 25: 2473–2479. https://doi.org/10.5194/nhess-25-2473-2025.

Giorgi, F., C. Torma, E. Coppola, N. Ban, C. Schär, and S. Somot. 2016. "Enhanced Summer Convective Rainfall at Alpine High Elevations in Response to Climate Warming." *Nature Geoscience* 9, no. 8: 584–589. https://doi.org/10.1038/ngeo2761.

Givon, Y., O. Hess, E. Flaounas, J. L. Catto, M. Sprenger, and S. Raveh-Rubin. 2024. "Process-Based Classification of Mediterranean Cyclones Using Potential Vorticity." *Weather and Climate Dynamics* 5: 133–162. https://doi.org/10.5194/wcd-5-133-2024.

GloH2O. 2020. "*MSWEP—Multi-Source Weighted-Ensemble Precipitation.*" https://www.gloh2o.org/mswep/.

Grazzini, F., G. C. Craig, C. Keil, G. Antolini, and V. Pavan. 2020. "Extreme Precipitation Events Over Northern Italy. Part I: A Systematic Classification With Machine-Learning Techniques." *Quarterly Journal of the Royal Meteorological Society* 146, no. 726: 69–85. https://doi.org/10.1002/qj.3635.

Harrington, L. J., P. B. Gibson, S. M. Dean, D. Mitchell, S. M. Rosier, and D. J. Frame. 2016. "Investigating Event-Specific Drought Attribution Using Self-Organizing Maps." *Journal of Geophysical Research: Atmospheres* 121, no. 21: 12,766–12,780. https://doi.org/10.1002/2016JD025602.

Hartmann, D. L. 2016. "Chapter 10—Climate Sensitivity and Feedback Mechanisms." In *Global Physical Climatology*, edited by D. L. Hartmann, Second ed., 293–323. BostonElsevier. https://doi.org/10.1016/B978-0-12-328531-7.00010-4.

Hersbach, H., B. Bell, P. Berrisford, et al. 2020. "The era5 Global Reanalysis." *Quarterly Journal of the Royal Meteorological Society* 146, no. 730: 1999–2049. https://doi.org/10.1002/qj.3803.

Hewitson, B., and R. Crane. 2002. "Self-Organizing Maps: Applications to Synoptic Climatology." *Climate Research* 22: 13–26. https://doi.org/10.3354/cr022013.

Holton, J. R., and G. J. Hakim. 2013. *An Introduction to Dynamic Meteorology*. Fifth ed. Accademic Press, Elsevier. https://doi.org/10.1016/C2009-0-63394-8.

Horton, D., N. Johnson, D. Singh, et al. 2015. "Contribution of Changes in Atmospheric Circulation Patterns to Extreme Temperature Trends." *Nature* 522: 465–469. https://doi.org/10.1038/nature14550.

Hussain, M., and I. Mahmud. 2019. "pyMannKendall: A Python Package for Non Parametric Mann Kendall Family of Trend Tests." *Journal of Open Source Software* 4, no. 39: 1556. https://doi.org/10.21105/joss.01556.

Huth, R., C. Beck, and M. Kucerova. 2016. "Synoptic-Climatological Evaluation of the Circulation Pattern Over Europe." *International Journal of Climatology* 36: 2710–2726. https://doi.org/10.1002/joc.4546.

Iannuccilli, M., G. Bartolini, G. Betti, et al. 2021. "Extreme Precipitation Events and Their Relationships With Circulation Types in Italy." *International Journal of Climatology* 41, no. 10: 4769–4793. https://doi.org/10.1002/joc.7109.

John, A., H. Douville, A. Ribes, and P. Yiou. 2022. "Quantifying CMIP6 Model Uncertainties in Extreme Precipitation Projections." *Weather and Climate Extremes* 36: 100435. https://doi.org/10.1016/j.wace.2022.100435.

Johnson, N. C., S. B. Feldstein, and B. Tremblay. 2008. "The Continuum of Northern Hemisphere Teleconnection Patterns and a Description of the Nao Shift With the Use of Self-Organizing Maps." *Journal of Climate* 21, no. 23: 6354–6371. https://doi.org/10.1175/2008JCLI2380.1.

Jones, S. 2024. "*Spain floods: searchers scour car parks and malls amid fears death toll will rise.*" https://www.theguardian.com/world/2024/nov/04/spain-floods-military-unit-searches-car-parks-and-malls-amid-fears-death-toll-will-rise.

Kohonen, T. 1982. "Self-Organized Formation of Topologically Correct Feature Maps." *Biological Cybernetics* 43, no. 1: 59–69. https://doi.org/10.1007/BF00337288.

Kohonen, T. 1998. "The Self-Organizing Map." *Neurocomputing* 21, no. 1: 1–6. https://doi.org/10.1016/S0925-2312(98)00030-7.

Kohonen, T. 2001. "The Basic SOM." In *Self-Organizing Maps*, edited by T. Kohonen, 105–176. Springer. https://doi.org/10.1007/978-3-642-56927-2_3.

Kurtz, T., and T. Martin. 2023. "Minisom Tutorial." *GitHub Repository*. https://github.com/taliakurtz/MiniSOM_tutorial.

Lavers, D. A., A. Simmons, F. Vamborg, and M. J. Rodwell. 2022. "An Evaluation of ERA5 Precipitation for Climate Monitoring." *Quarterly Journal of the Royal Meteorological Society* 148, no. 748: 3152–3165. https://doi.org/10.1002/qj.4351.

Lenderink, G., R. Barbero, J. M. Loriaux, and H. J. Fowler. 2017. "Super-Clausius–Clapeyron Scaling of Extreme Hourly Convective Precipitation and Its Relation to Large-Scale Atmospheric Conditions." *Journal of Climate* 30, no. 15: 6037–6052. https://doi.org/10.1175/JCLI-D-16-0808.1.

Liu, Y., and R. H. Weisberg. 2011. "A Review of Self-Organizing Map Applications in Meteorology and Oceanography." In *Self Organizing Maps—Applications and Novel Algorithm Design*, edited by J. I. Mwasiagi, 253–272. IntechOpen. https://doi.org/10.5772/13146.

Lorenz, E. N. 1969. "Atmospheric Predictability as Revealed by Naturally Occurring Analogues." *Journal of the Atmospheric Sciences* 26, no. 4: 636–646. https://doi.org/10.1175/1520-0469(1969)26%3C636:APARBN%3E2.0.CO;2.

Mastrantonas, N., L. Furnari, L. Magnusson, et al. 2022. "Forecasting Extreme Precipitation in the Central Mediterranean: Changes in Predictors' Strength With Prediction Lead Time." *Meteorological Applications* 29, no. 6: e2101. https://doi.org/10.1002/met.2101.

Mastrantonas, N., P. Herrera-Lormendez, L. Magnusson, F. Pappenberger, and J. Matschullat. 2021. "Extreme Precipitation Events in the Mediterranean: Spatiotemporal Characteristics and Connection to Large-Scale Atmospheric Flow Patterns." *International Journal of Climatology* 41, no. 4: 2710–2728. https://doi.org/10.1002/joc.6985.

Mazza, E., U. Ulbrich, and R. Klein. 2017. "The Tropical Transition of the October 1996 Medicane in the Western Mediterranean Sea: A Warm Seclusion Event." *Monthly Weather Review* 145, no. 7: 2575–2595. https://doi.org/10.1175/MWR-D-16-0474.1.

Mazzarella, A., M. Manlio, and G. Tranfaglia. 2002. "The Latest Flood Event of 4-5 May 1998 in the Sarno Area and the Inadequate Resolution of the Rain-Gauge Network." *Quaderni di Geologia Applicata* 7, no. 2: 203–211. In Italian.

Michelangeli, P. A., R. Vautard, and B. Legras. 1995. "Weather Regimes: Recurrence and Quasi Stationarity." *Journal of Atmospheric Sciences* 52, no. 8: 1237–1256. https://doi.org/10.1175/1520-0469(1995)052%3C1237:WRRAQS%3E2.0.CO;2.

Miglietta, M. M., and S. Davolio. 2022. "Dynamical Forcings in Heavy Precipitation Events Over Italy: Lessons From the HyMeX SOP1 Campaign." *Hydrology and Earth System Sciences* 26, no. 3: 627–646. https://doi.org/10.5194/hess-26-627-2022.

10970088, 2025, 15, Downloaded from https://rmets.onlinelibrary.wiley.com/doi/10.1002/joc.70118 by CochraneItalia, Wiley Online Library on [03/12/2025]. See the Terms and Conditions (https://onlinelibrary.wiley.com/terms-and-conditions) on Wiley Online Library for rules of use; OA articles are governed by the applicable Creative Commons License

Mittermeier, M., M. Braun, M. Hofstätter, Y. Wang, and R. Ludwig. 2019. "Detecting Climate Change Effects on Vb Cyclones in a 50-Member Single-Model Ensemble Using Machine Learning." *Geophysical Research Letters* 46, no. 24: 14653–14661. https://doi.org/10.1029/2019GL084969.

Montani, A., C. Marsigli, F. Nerozzi, T. Paccagnella, S. Tibaldi, and R. Buizza. 2003. "The Soverato Flood in Southern Italy: Performance of Global and Limited-Area Ensemble Forecasts." *Nonlinear Processes in Geophysics* 10, no. 3: 261–274. https://doi.org/10.5194/npg-10-261-2003.

Moore, B., M. Winsor, and C. Alcini. 2024. "*Spain Flooding Death Toll Climbs to 217 as Cleanup Efforts in Mud-Soaked Streets Continue.*" https://abcnews.go.com/International/spain-flooding-death-toll-climbs-211-clean-efforts/story?id=115432458.

National Academies of Sciences, Engineering, and Medicine. 2016. *Attribution of Extreme Weather Events in the Context of Climate Change*. National Academies Press. https://doi.org/10.17226/21852.

Nuissier, O., B. Joly, A. Joly, V. Ducrocq, and P. Arbogast. 2011. "A Statistical Downscaling to Identify the Large-Scale Circulation Patterns Associated With Heavy Precipitation Events Over Southern France." *Quaterly Journal of the Royal Meteorological Society* 137, no. 660: 1812–1827. https://doi.org/10.1002/qj.866.

Odoulami, R. C., P. Wolski, and M. New. 2023. "Attributing the Driving Mechanisms of the 2015–2017 Drought in the Western Cape (South Africa) Using Self-Organising Maps." *Environmental Research Letters* 18: 074043. https://doi.org/10.1088/1748-9326/ace26f.

O'Gorman, P. A. 2015. "Precipitation Extremes Under Climate Change." *Current Climate Change Reports* 1, no. 2: 49–59. https://doi.org/10.1007/s40641-015-0009-3.

O'Gorman, P. A., and T. Schneider. 2009. "The Physical Basis for Increases in Precipitation Extremes in Simulations of 21st-Century Climate Change." *Proceedings of the National Academy of Sciences of the United States of America* 106, no. 35: 14773–14777. https://doi.org/10.1073/pnas.0907610106.

Otto, F. E. L. 2017. "Attribution of Weather and Climate Events." *Annual Review of Environment and Resources* 42: 627–646. https://doi.org/10.1146/annurev-environ-102016-060847.

Pall, P., M. R. Allen, and D. A. Stone. 2007. "Testing the Clausius–Clapeyron Constraint on Changes in Extreme Precipitation Under CO_2 Warming." *Climate Dynamics* 28, no. 4: 351–363. https://doi.org/10.1007/s00382-006-0180-2.

Pavan, V., G. Antolini, G. Agrillo, et al. 2013. "The ARCIS Project." *Italian Journal of Agrometeorology* 2: 51–55.

Pavan, V., G. Antolini, R. Barbiero, et al. 2019. "High Resolution Climate Precipitation Analysis for North-Central Italy, 1961–2015." *Climate Dynamics* 52, no. 5: 3435–3453. https://doi.org/10.1007/s00382-018-4337-6.

Pfahl, S., P. A. O'Gorman, and E. M. Fischer. 2017. "Understanding the Regional Pattern of Projected Future Changes in Extreme Precipitation." *Nature Climate Change* 7, no. 6: 423–427. https://doi.org/10.1038/nclimate3287.

Philipp, A., J. Bartholy, C. Beck, et al. 2010. "Cost733cat—A Database of Weather and Circulation Type Classifications." *Physics and Chemistry of the Earth* 35, no. 9: 360–373. https://doi.org/10.1016/j.pce.2009.12.010.

Prete, M., F. Guadagno, and A. Hawkins. 1998. "Preliminary Report on the Landslides of 5 May 1998, Campania, Southern Italy." *Bulletin of Engineering Geology and the Environment* 57, no. 2: 113–129. https://doi.org/10.1007/s100640050028.

Ramos, M., D. Barriopedro, and E. Dutra. 2015. "Circulation Weather Types as a Tool in Atmospheric, Climate, and Environmental Research." *Frontiers in Environmental Science* 3, no. 44: 3. https://doi.org/10.3389/fenvs.2015.00044.

Ridal, M., E. Bazile, P. Le Moigne, et al. 2024. "CERRA, the Copernicus European Regional Reanalysis System." *Quarterly Journal of the Royal Meteorological Society* 150, no. 763: 3385–3411. https://doi.org/10.1002/qj.4764.

Schimanke, S., M. Ridal, P. Le Moigne, et al. 2021. "*Cerra sub-daily regional reanalysis data for europe on single levels from 1984 to present*. Copernicus Climate Change Service (C3S) Climate Data Store (CDS)." https://doi.org/10.24381/cds.622a565a.

Seneviratne, S., X. Zhang, M. Adnan, et al. 2021. "Weather and Climate Extreme Events in a Changing Climate." In *Climate Change 2021: The Physical Science Basis. Contribution of Working Group I to the Sixth Assessment Report of the Intergovernmental Panel on Climate Change. Cambridge, United Kingdom and New York*, edited by V. Masson-Delmotte, P. Zhai, A. Pirani, S. Connors, C. Péan, and S. Berger, 1513–1766. Cambridge University Press. https://doi.org/10.1017/9781009157896.013.

Shepherd, T. G. 2014. "Atmospheric Circulation as a Source of Uncertainty in Climate Change Projections." *Nature Geoscience* 7, no. 10: 703–708. https://doi.org/10.1038/ngeo2253.

Sheridan, S., and C. Lee. 2011. "The Self-Organizing Map in Synoptic Climatological Research." *Progress in Physical Geography* 35, no. 1: 109–119. https://doi.org/10.1177/0309133310397582.

Sioni, F., S. Davolio, F. Grazzini, and L. Giovannini. 2023. "Revisiting the Atmospheric Dynamics of the Two Century Floods Over North-Eastern Italy." *Atmospheric Research* 286: 106662. https://doi.org/10.1016/j.atmosres.2023.106662.

Spuler, F. R., M. Kretschmer, Y. Kovalchuk, M. A. Balmaseda, and T. G. Shepherd. 2024. "Identifying Probabilistic Weather Regimes Targeted to a Local-Scale Impact Variable." *Environmental Data Science* 3: e25. https://doi.org/10.1017/eds.2024.29.

Stryhal, J., and E. Plavcová. 2023. "On Using Self-Organizing Maps and Discretized Sammon Maps to Study Links Between Atmospheric Circulation and Weather Extremes." *International Journal of Climatology* 43, no. 6: 2678–2698. https://doi.org/10.1002/joc.7996.

Swales, D., M. Alexander, and M. Hughes. 2016. "Examining Moisture Pathways and Extreme Precipitation in the U.S. Intermountain West Using Self-Organizing Maps." *Geophysical Research Letters* 43, no. 4: 1727–1735. https://doi.org/10.1002/2015GL067478.

Trenberth, K. E. 1999. "Conceptual Framework for Changes of Extremes of the Hydrological Cycle With Climate Change." *Climatic Change* 42: 327–339. https://doi.org/10.1023/A:1005488920935.

Trigo, I. F., G. R. Bigg, and T. D. Davies. 2002. "Climatology of Cyclogenesis Mechanisms in the Mediterranean." *Monthly Weather Review* 130, no. 3: 549–569. https://doi.org/10.1175/1520-0493(2002)130%3C0549:COCMIT%3E2.0.CO;2.

Vallorani, R., G. Bartolini, G. Betti, et al. 2018. "Circulation Type Classifications for Temperature and Precipitation Stratification in Italy." *International Journal of Climatology* 38: 915–931. https://doi.org/10.1002/joc.5219.

Vautard, R., and P. Yiou. 2009. "Control of Recent European Surface Climate Change by Atmospheric Flow." *Geophysical Research Letters* 36: L22702. https://doi.org/10.1029/2009GL040480.

Vautard, R., P. Yiou, F. Otto, et al. 2016. "Attribution of Human-Induced Dynamical and Thermodynamical Contributions in Extreme Weather Events." *Environmental Research Letters* 11, no. 11: 114009. https://doi.org/10.1088/1748-9326/11/11/114009.

Yiou, P., A. Jézéquel, P. Naveau, F. E. L. Otto, R. Vautard, and M. Vrac. 2017. "A Statistical Framework for Conditional Extreme Event Attribution." *Advances in Statistical Climatology, Meteorology and Oceanography* 3: 17–31. https://doi.org/10.5194/ascmo-3-17-2017.

Yiou, P., R. Vautard, and C. Cassou. 2007. "Inconsistency Between Atmospheric Dynamics and Temperatures During the Exceptional 2006/2007 Fall/Winter and Recent Warming in Europe." *Geophysical Research Letters* 34: L21808. https://doi.org/10.1029/2007GL031981.

10970088, 2025, 15, Downloaded from https://rmets.onlinelibrary.wiley.com/doi/10.1002/joc.70118 by CochraneItalia, Wiley Online Library on [03/12/2025]. See the Terms and Conditions (https://onlinelibrary.wiley.com/terms-and-conditions) on Wiley Online Library for rules of use; OA articles are governed by the applicable Creative Commons License

Supporting Information

Additional supporting information can be found online in the Supporting Information section. **Data S1:** Supporting Information.

Appendix A

Self-Organising Maps

The Self-Organising Map (SOM) (Kohonen 1982, 1998, 2001) is an effective tool for the visualisation of high-dimensional data. This algorithm converts complex, nonlinear statistical relationships into simple geometric relationships through a nonparametric regression process (Kohonen 1998) while preserving the topology and structure of the data. Given an N-dimensional cloud of data points, the SOM positions a set number of nodes within the data space so that their distribution reflects the underlying multi-dimensional data distribution (Hewitson and Crane 2002). Topology preservation ensures that similar data points in the high-dimensional space remain close together in the lower-dimensional representation. This allows SOMs to maintain meaningful patterns, facilitate cluster identification, and provide a smooth, interpretable mapping of the data, making them valuable for exploratory analysis and visualisation. Unlike traditional clustering algorithms, which directly partition data into discrete groups, SOMs map data onto a grid where each node represents a nearby set of observations. This approach preserves the relationships between similar data points, allowing for the identification of patterns in complex datasets. While SOM analysis often results in some form of clustering, its primary objective is to approximate the overall multi-dimensional data distribution rather than explicitly define clusters (Hewitson and Crane 2002). Because of the topological structure of the nodes, some clusters in a SOM may be more similar to each other than others, forming a continuous distribution rather than strictly separated categories.

SOM Preprocessing

The SOM is applied to stacked, standardised, daily anomalies of Z500 (deseasonalised and detrended) and mSLP (deseasonalised) retrieved from ERA5, defined over a (52°N-27°N, 13°W-35°E) domain and associated with EPEs. First, we compute the daily average of each variable. Then we subtract the seasonal climatology, removing from each variable the 45-day running mean, and for Z500 we additionally apply a linear detrending. We select the subset relative only to EPEs. First, we perform a 70–30 split for the training and test set—that is the first 70% of the dataset is the training set, and the last 30% is the test set. Then, each variable is separately standardised through the `StandardScaler()` function of the *sklearn.preprocessing* module. Finally, these two variables are stacked to obtain, for each extreme day, a combined map of Z500 and mSLP anomalies. Lastly, we perform a data reduction by principal component analysis (PCA) in S-mode before applying our clusterisation algorithm and we weight the input data by the square root of the cosine of latitude.

To explain in more detail why the PCA step is necessary, we now consider the example of the ArCIS dataset used during the validation over North-Central Italy. For this dataset we identify 674 EPEs and the two variables, Z500 and mSLP, have each size of (101, 193). Therefore, the dataset on which we should apply the SOM has a dimension of (674, 2×101×193) or equivalently (674, 38′986), This translates into 674 observations and 38′986 features. Moreover, the training dataset reduces into 472 observations after the training-set split. As a results, the number of observations is way too small in comparison with the number of features and data reduction becomes essential to avoid the *curse of dimensionality*. This concept, introduced by Richard E. Bellman (Bellman 1961, 1984), describes the exponential increase in computational complexity that occurs as dimensionality grows. This problem can lead to difficulties for the SOM to identify meaningful cluster and to computational expensive calculations. Kohonen himself warns that preprocessing should not be overlooked when using SOMs (Kohonen 2001). For this reason, following the approach of Federico et al. (2008), we perform a data reduction by PCA in S-mode. When applying S-mode PCA to a matrix, the grid point (features) are treated as variables, while the days correspond to observations. Consequently, the linear relationships identified by PCA are between the time series of the grid points. Moreover, we retain the number of components explaining 95% of the total field variance since a sensitivity analysis found no benefit in increasing the number of PCA components.

We train the SOM on the training set (the first 70% of the dataset) and then we apply the trained SOM on the entire dataset. The test set is used here to evaluate and assess the quality of the SOM and to choose the optimal configuration. For the computation of the composites, all available data is considered.

Selecting SOM Hyperparameters

The Self-Organising Maps (SOM) algorithm is characterised by a number of hyperparameters that must be selected by the user.

Two typical metrics are used to monitor and asses the quality of the SOMs: *quantization* and *topographic errors*. The quantization error reflects the degree of separation between the data points and the map's prototypes (the clusters obtained by the SOM, also referred to as *best-matching unit*), while the topographic error measures the accuracy of the maps in preserving the topology (Kohonen 2001). For both metrics, lower values indicate better performance, with a topographic error of zero indicating a perfect topographic representation. Since selecting different parameters can result in slightly different outcomes, it is common practice to generate multiple SOMs and select the configuration that minimises both quantization and topographic errors. In this study, as in Stryhal and Plavcová (2023), the quantization error represents the Euclidean distance between each circulation map and its best-matching unit, averaged over all clusters, while the topological error is the percentage of circulation maps whose best-matching unit and second-best-matching unit are not adjacent in the SOM array. The first hyperparameter we select is the size of the network, after physical and practical consideration already enlighted in Section 2.2 that is 2×2 for North Central Italy and 2×3 for all the peninsula. Then we tested all available neighbourhood functions (*Gaussian*, *Bubble*, *Mexican hat* and *Triangle*) and the quantization and topographic error were evaluated on the test set and minimised. We found that the *Gaussian* neighbourhood function consistently provided the lowest errors across all trials. Additionally, various configurations of sigma and learning rate were tested in the same way to optimise the performance further. We found that in the North-Central analysis, there was some fluctuation in the selection of the optimal parameter, whereas the results remained consistent when extending the analysis to the whole of Italy. However, this does not compromise the quality of our work since similar results for North Central Italy were obtained considering the different configurations. Moreover, the validation over North-Central Italy represents a preliminary step rather than the final outcome. This difference, however, is probably due to the fact that we have way more EPEs when considering all Italy rather than just a portion. In the end, we considered the configuration shown in Table A1. We generate 10 SOMs with this configuration and select the one with the lowest quantization error (the *Master* SOM) as the "best" for defining the WTs.

TABLE A1 | SOM configuration.

Domain	Row by col	Neighbourhood function	Sigma	Learning rate	Decay function
North-Central Italy[a]	2×2	Gaussian	1	0.002	`asymptotic_decay`
Italy[b]	2×3	Gaussian	1	0.005	`asymptotic_decay`

[a]Same for ArCIS, CERRA and MSWEP.
[b]For CERRA, extended to all Italy.

10970088, 2025, 15, Downloaded from https://rmets.onlinelibrary.wiley.com/doi/10.1002/joc.70118 by CochraneItalia, Wiley Online Library on [03/12/2025]. See the Terms and Conditions (https://onlinelibrary.wiley.com/terms-and-conditions) on Wiley Online Library for rules of use; OA articles are governed by the applicable Creative Commons License